FINAL REPORT

ATS-5 RANGING RECEIVER AND L-BAND EXPERIMENT

VOLUME I

APPLICATIONS TECHNOLOGY SATELLITE PROGRAM

CONTRACT NAS 5-21019

SEPTEMBER 1971

PREPARED FOR

NATIONAL AERONAUTICS AND SPACE ADMINISTRATION

GODDARD SPACE FLIGHT CENTER

GREENBELT, MARYLAND

PREPARED BY

WESTINGHOUSE ELECTRIC CORPORATION

DEFENSE AND SPACE CENTER

BALTIMORE, MARYLAND

1. Report No.	2. Government Accession No.	3. Recipient's Catalog No.

4. Title and Subtitle	5. Report Date
FINAL REPORT ATS-5 RANGING RECEIVER AND L-BAND EXPERIMENT VOLUME I	September 1971
	6. Performing Organization Code
7. Author(s)	8. Performing Organization Report No.
9. Performing Organization Name and Address Westinghouse Electric Corporation Defense and Space Center Baltimore, Maryland 21203	10. Work Unit No.
	11. Contract or Grant No. NAS 5-21019
12. Sponsoring Agency Name and Address NASA/GSFC Greenbelt, Maryland	13. Type of Report and Period Covered Final
	14. Sponsoring Agency Code

15. Supplementary Notes

16. Abstract

The ATS-5 Ranging Receiver and L-band Experiment Final Report contains information describing the L-band ranging receiver and preliminary results of test data obtained at the Mojave station. Also covered in this report is a brief program history and description of the installation and testing phase of the program at Mojave Ground Station.

The ranging receiver was designed to utilize tone ranging techniques, with the tones being supplied from the station ATS ranging system. The receiver is used in conjunction with the station L-band transmit/receive system.

The majority of the ranging and position location data which was obtained with the receiver will be analyzed and presented in volume II of this report.

17. Key Words (Selected by Author(s))	18. Distribution Statement
ATS-5 Ranging Receiver and L-Band Experiment Volume I	

19. Security Classif. (of this report)	20. Security Classif. (of this page)	21. No. of Pages	22. Price*
U	U	56	

*For sale by the Clearinghouse for Federal Scientific and Technical Information, Springfield, Virginia 22151.

TABLE OF CONTENTS

LIST OF ILLUSTRATIONS

LIST OF TABLES

SECTION 1

INTRODUCTION

1.1 PROGRAM HISTORY

1.1.1 Pre-Launch Plan

Prior to the launch of ATS-5, (ATS-E) investigations were made into ranging and aircraft tracking at L-band frequencies. An experiment proposal* was prepared and submitted which was designed to evaluate propagation effects at L-band frequencies on ranging accuracy as well as multiple aircraft ranging and communications. The major objectives of the experiment were:

1. To evaluate the effects of propagation on tone ranging at L-band frequencies.
2. To perform position location experiments from Mojave to an aircraft and a simulated aircraft.
3. To perform a preliminary evaluation of the PLACE concept which provides turnaround ranging and voice communications to multiple aircraft.

To meet the above objectives a series of experiments were outlined and the conceptual design of the necessary equipment for the experiment was developed. The system block diagram, figure 1.1, illustrates the total experiment configuration and indicates the interfacing between station equipment and experiment equipment. The following individual experiments were to be performed:

a. Comparisons of simultaneous L-band range measurements and C-band range measurements with spacecraft ephemeris data for corresponding time periods.
b. Turnaround ranging to an aircraft using the C- to L-band cross-strap mode from the ground station to ATS-5 to aircraft link and L- to C-band cross-strap on the return link.

---

*"Proposal for L-band Ranging and Position Location Experiment," Westinghouse Electric Corporation, 14 July 1969, p. 2-1.

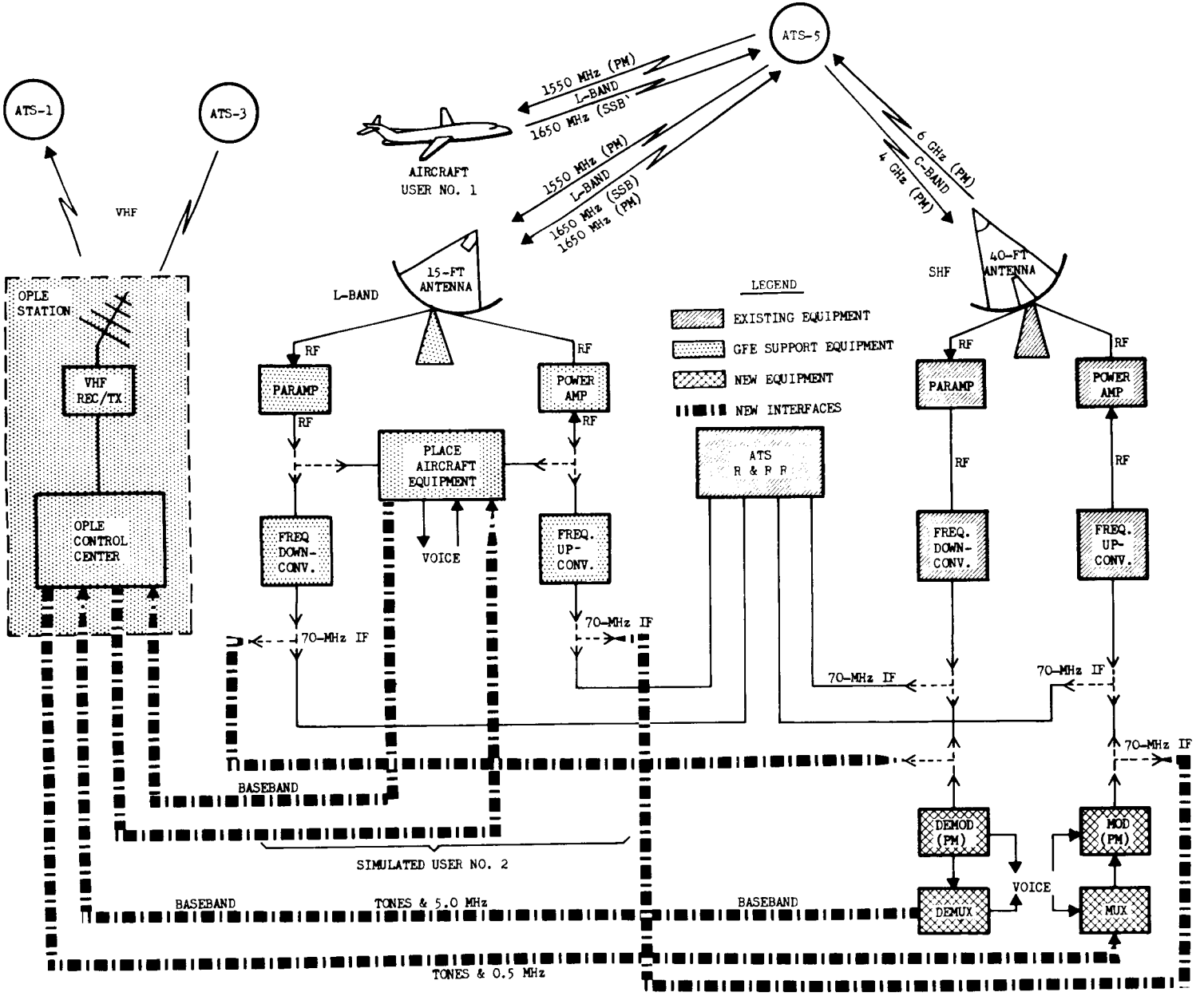

Figure 1.1 Mojave Station Ranging and Position Location Equipment System Block Diagram

c. Position location of an aircraft and a simulated aircraft using the ranging link described in b. above with the ATS Ranging (ATSR) system for one circle of position and the modified OPLE equipment and ATS-1 or ATS-3 for the second circle of position.

The equipment which was originally proposed to implement the experiment plan consisted of a modulator and a demodulator which would interface with the Mojave station equipment at 70 MHz. The modulator phase modulated four subcarrier voice channels and the OPLE ranging tones on a 70-MHz carrier which would then interface with the station equipment for up-conversion to C-band.

This C-band signal was transmitted to ATS-5, where it was translated to L-band. An aircraft or simulated aircraft received this signal, processed it, and retransmitted it as a single-sideband L-band signal. The aircraft signal was received by ATS-5, which was in the multiple access L- to C-band cross-strap mode, and retransmitted to the ground station.

The demodulator interfaced at 70 MHz with the station C-band down-converter and carrier tracked the received signal. Following the 70-MHz track channel were four channels of coherent subcarrier voice demodulators and an OPLE range tone extractor. The OPLE range tones were transferred to the modified OPLE equipment, where a range determination was performed.

1.1.2 Post-Launch Plan

Soon after the launch of ATS-5, problems were encountered which prevented extending of the gravity gradient booms to stabilize the spacecraft. Instead, the spacecraft achieved a spin-stabilized orbit which caused the L-band directional antenna to sweep across the surface of the Earth at a 77-sweep-per-minute rate rather than providing constant illumination of the Earth's surface, as planned. This produced an illumination period (between the 3-dB points of the spacecraft antenna) of 60 milliseconds.

Since the proposed equipment for the L-band experiment was intended to operate under steady-state signal conditions, a re-evaluation of the experiment and hardware was necessary. It was determined that the OPLE equipment could not be modified to operate under the pulsed signal conditions that existed. Modification of the ATSR to provide the required ranging data proved to be undesirable.

A study of the program objectives and spacecraft capabilities was made with a view to re-orienting the program to obtain the most useful information under the funding constraints of the contract. This study disclosed that none of the original

objectives could be completely realized, but that objectives 1 and 2 could be partially realized. It was decided that objectives 1 and 2 would be modified as follows:

1. Evaluate the effects of propagation on tone ranging at L-band frequencies under the limitation imposed upon the data by the spacecraft spin.
2. Perform a two-satellite position location experiment of a simulated user, such as the Mojave station, using one-way ranging.

Secondary objectives were also established for the program as follows:

1. Evaluate the effects of multipath interference on tone ranging signals at L-band.
2. Evaluate the effects of propagation on tone ranging signals at VHF.
3. Evaluate station-to-station tone ranging using high stability frequency standards at each station.

In order to meet the revised objectives a new system configuration was developed (see figure 1.2) in which the ATSR equipment was used in conjunction with a newly designed ranging receiver. The ATSR ranging equipment supplied a range tone modulated 70-MHz carrier which interfaced with the station L-band up-converter and L-band transmitter. The range tone modulation was either 4 kHz or 20 kHz. The L-band signal was transmitted at 1651 MHz to the ATS-5 spacecraft, where it was translated to 1550 MHz and retransmitted to the earth station. The 1550-MHz signal was received by the station L-band receiver and down-converted to 70 MHz to interface with the ranging receiver.

The ranging receiver consisted of three major components: a carrier track unit, range demodulator, and a paper tape punch unit. The carrier track unit was similar to that originally proposed, but was modified to acquire and track a pulsed 70-MHz carrier. The range demodulator was designed to accept the pulsed range tone signal from the carrier track unit and process it to provide a useful range measurement. This range measurement was then recorded along with time of day on punched paper tape.

1.2 PROGRAM SUMMARY

The ATS-5 L-band ranging and position location experiment as originally conceived could not be implemented due to the failure of ATS-5 to achieve a gravity gradient stabilized configuration. It was necessary to revise both the original experiments and the equipment required to perform the experiments. The equipment changes required were (1) modify the carrier track unit design to acquire and track a pulsed down link signal from ATS-5 and (2) design a range demodulator to provide useful

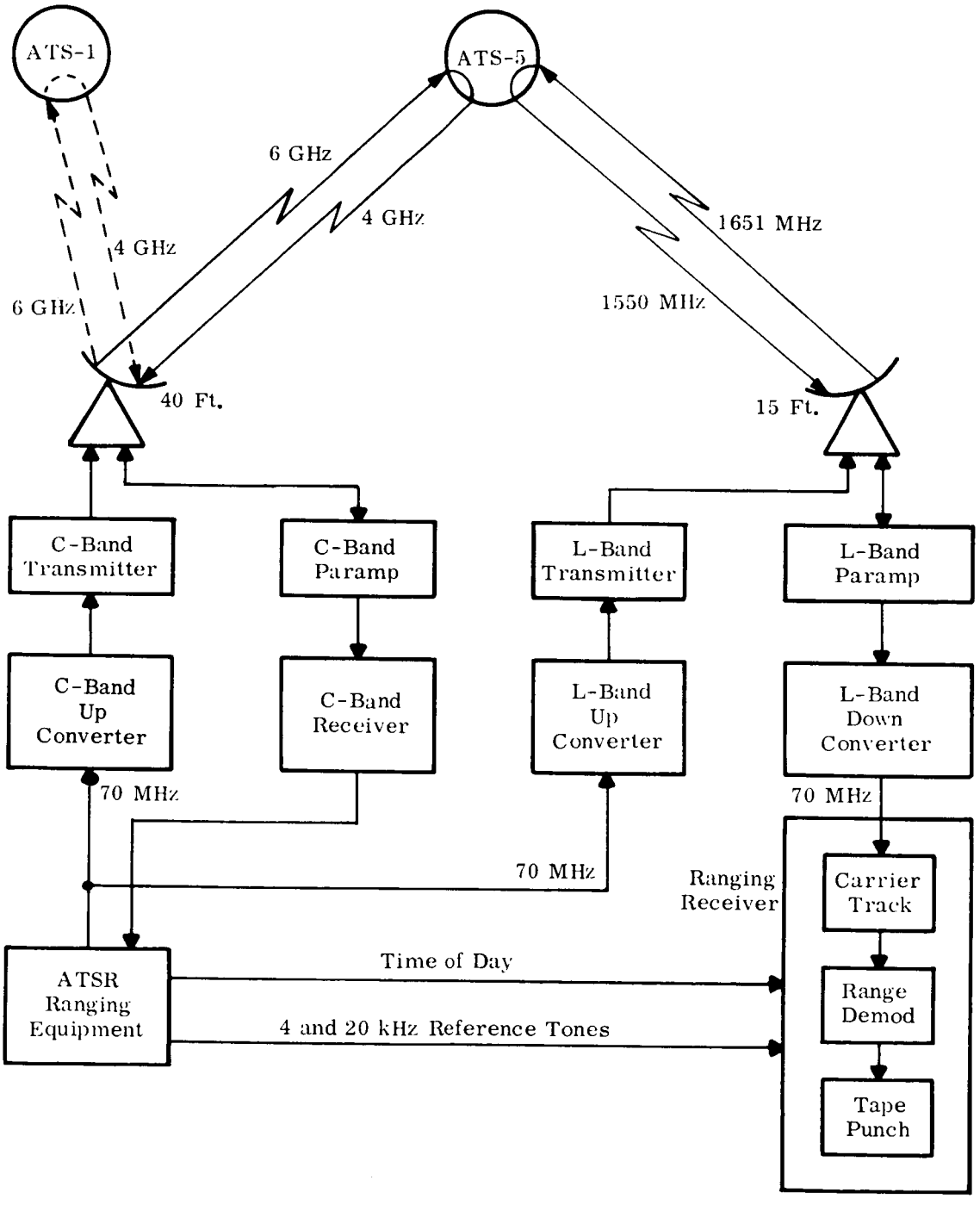

Figure 1.2 Post-Launch Basic L-Band Experiment Configuration

range information from this pulsed signal. The range demodulator was required because neither the OPLE ranging equipment nor the ATSR ranging equipment could be used with the pulsed signal received from the spacecraft.

An experiment plan was prepared to perform the various tests under the link conditions which existed, using the newly designed ranging equipment. The ranging equipment (or ranging receiver as it has been designated) was fabricated and tested prior to shipment to the Mojave earth station. In early January 1971 the ranging receiver was shipped to Mojave, installed and acceptance tested. During this period several interface problems were resolved and minor modifications were made to the ranging receiver to simplify future testing.

The individual tests outlined in the experiment plan were performed and an operations plan was prepared to provide the site personnel with a procedure to follow during future testing. Only the initial experiment checkout data results are included in this report. Data which was acquired after the initial experiment checkout phase will be covered by the Data Reduction and Analysis effort under another contract.

SECTION 2

EXPERIMENT EQUIPMENT

2.1 DESIGN PHILOSOPHY

2.1.1 Ranging Receiver

A first step in determining the design parameter requirements for the ranging receiver was the calculation of the various link configurations which might be encountered. A tabulation of the links follows (table 2.1) which indicates that the weakest link, and consequently the one which would establish the equipment design criterion, is the spacecraft-to-aircraft link. This link, under the given conditions, would produce an unmodulated carrier signal at the aircraft with a carrier power to noise per unit bandwidth ratio of 46 dB.

2.1.2 Tracking Loop Design

Using the aircraft link from table 2.1 as the constraining link and subtracting 3 dB for design margin, a C/N_0 of 43 dB is arrived at. If a peak modulation index of 1.4 is assumed, carrier suppression due to modulation will be in the order of 5 dB. This means that the C/N_0 available to the tracking loop is in the order of 38 dB. This is the nominal signal level around which the carrier tracking loop was designed.

Since an aircraft with a directional antenna was to be used in the experiment, wide variations in signal level and track loop operation near threshold could be expected due to aircraft manuevering. Examining the performance characteristics of various tracking loop designs in light of the expected signal conditions led to the selection of a Jaffe-Rechtin design. * This design yields near optimum performance over a wide range of signal and noise levels. Although the loop settling time (for comparable bandwidths) is not as fast as the Minimum Lead Design, (*) the threshold performance is superior. A simplified diagram of the loop is shown in figure 2.1.

---

*Jaffe, L., and E. Rechtin, "Design and Performance of Phase-Lock Loops capable of near Optimum Performance Over a wide range of Input Signal and Noise Levels," Trans. IRE pp. 66-76, March 1955

(*) See Glossary

TABLE 2.1 LINK CALCULATIONS

	Up-Link 1.65 GHz		
	From Mojave	From Mojave	From Aircraft
Transmitter power output (dBm)	+60.0	+60.0	+53.0
Transmit antenna gain, net (dB)	+32.0	+32.0	+13.0
Receive antenna gain, net (dB)	+12.5	+12.5	+12.5
Total Gains	+104.5	+104.5	+78.5
Free space loss (dB)	-189.0	-189.0	-189.0
Received carrier power (dBm)	-84.5	-84.5	-110.5
S/C receiver noise temp (1780°/K) (dB)	32.5	32.5	32.5
Received noise power density (dBm/Hz)	-166.0	-166.0	-166.0
Cxr. -to-Noise per unit B.W. (C/N_o in dB)	+81.5	+81.5	+55.5

	Down-Link 1.55 GHz		
	To Mojave	To Aircraft	To Mojave
Transmitter power output (1-TWT) (dBm)	+41.0	+41.0	+33.5*
Transmit antenna gain, net (dB)	+12.5	+12.5	+12.5
Receive antenna gain, net (dB)	+33.5	+14.5	+33.5
Total Gains (dB)	+87.0	+68.0	+79.5
Free space loss (dB)	-188.5	-188.5	-188.5
Received carrier power (dBm)	-101.5	-120.5	-109.0
Receiver noise temp. (dB)	25.5	32.0	25.5
Received noise power density (dBm/Hz)	-173.0	-166.6	-173.0
Cxr. -to-noise per unit B.W. (C/N_o in dB)	+71.5	+46.1	+64.0
Overall link C/N_o	+71.0	+46.0	+55.0

*7.5 dB down due to transponder not being saturated.

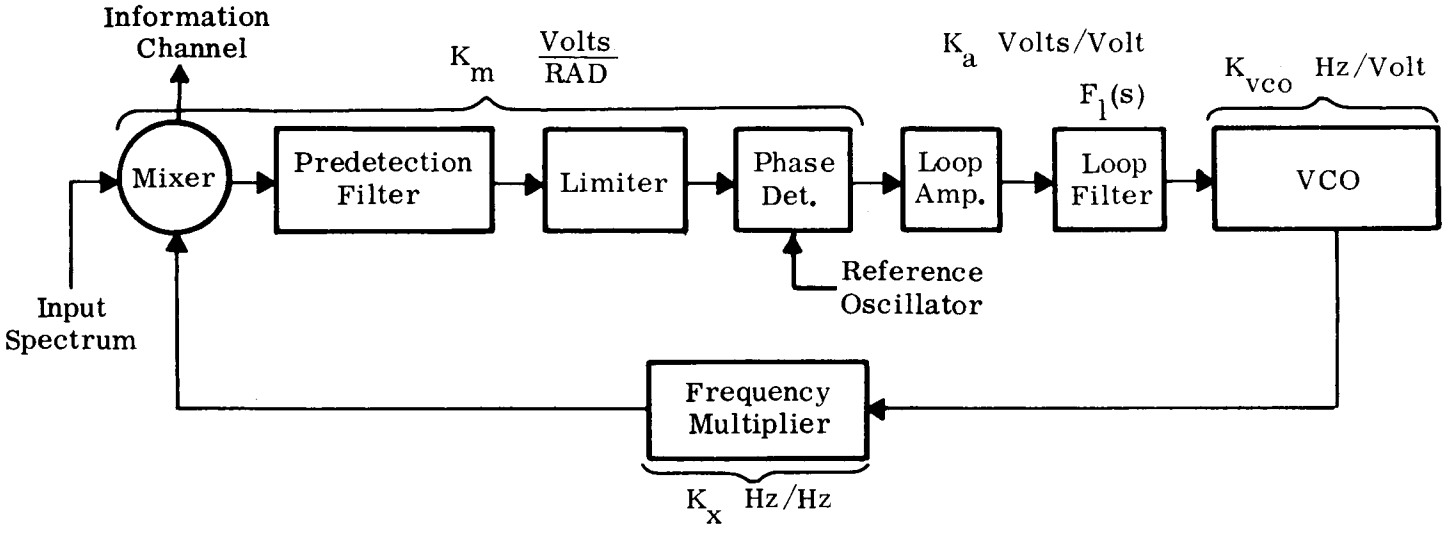

Figure 2.1 Carrier Track Loop Block Diagram

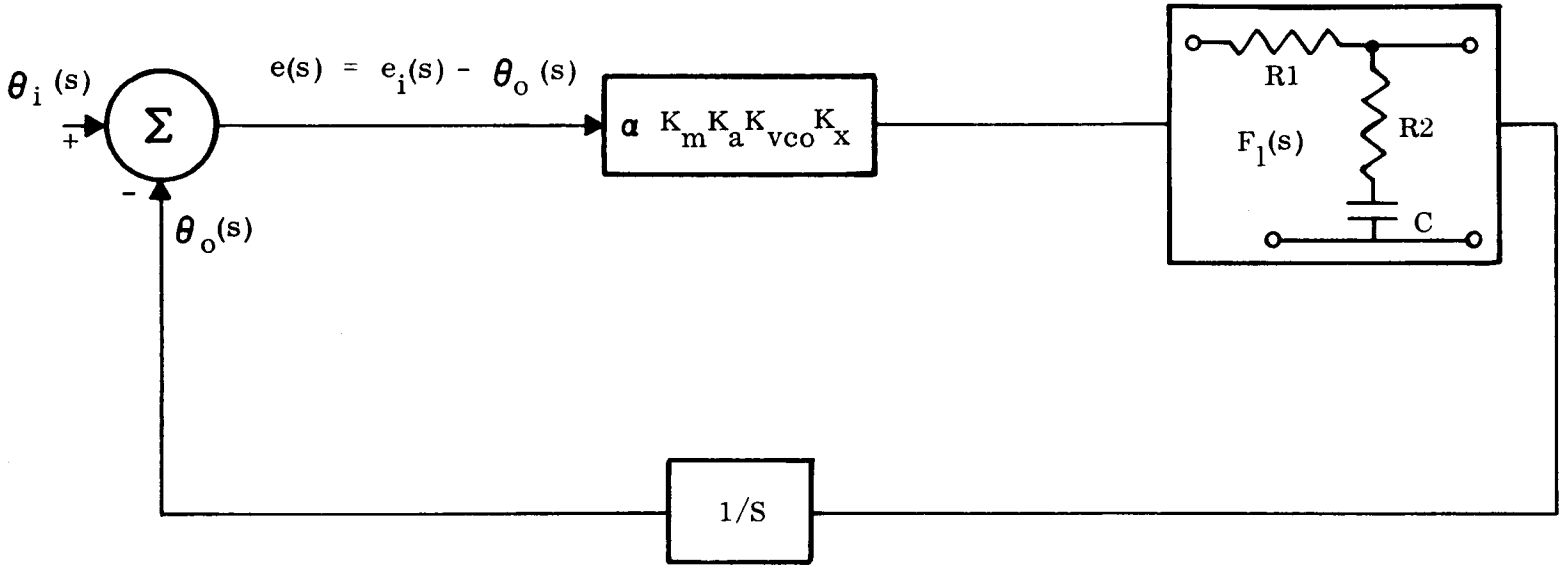

Figure 2.2 Carrier Track Loop, Linear Phase Model

The transfer function of the predetection unit (mixer, predetection filter, limiter RF amplifier) contributes to the phase detector scale factor. As a result, the diagram can be further simplified to the linear phase model shown in figure 2.2.

Table 2.2 lists each parameter, its dimension and definition.

The open loop gain is expressed in terms of the loop parameters as shown in equation 1.

$$G_o = 2 K_a K_m K_{vco} K_x \tag{1}$$

The loop filter time constants are a function of loop gain and the loop natural resonant frequency as shown by equations 2 through 4.

$$F_1(s) = \frac{\frac{S}{W_2} + 1}{\frac{S}{W_1} + 1} \tag{2}$$

$$T_1 = \frac{G_o}{B_o^2} \tag{3}$$

$$T_2 = \frac{\sqrt{2}}{B_o} \tag{4}$$

The open loop transfer function is indicated by equation 5.

$$H_o(s) = \frac{\theta_o(s)}{e(s)} = \frac{G_o F_1(s)}{S} = \frac{B_o^2 \left(1 + \frac{\sqrt{2}\, S}{B_o}\right)}{S^2} \tag{5}$$

The closed loop transfer function becomes:

$$H(s) = \frac{H_o(s)}{1 + H_o(S)} = \frac{1 + \frac{\sqrt{2}\, S}{B_o}}{\frac{S^2}{B_o^2} + \frac{\sqrt{2}\, S}{B_o} + 1} = \frac{\theta_o(s)}{\theta_i(s)} \tag{6}$$

The two-sided loop noise bandwidth expressed in terms of the closed loop transfer function is given by equation 7.

$$2 B L O = \frac{1}{2\pi j\infty} \int_{-j\infty}^{+j\infty} \left| H(s) \right|^2 ds \tag{7}$$

TABLE 2.2 NOMENCLATURE

Parameters	Dimension	Definition
K_m	volts/rad	Phase detector constant
K_a	volts/volt	Loop amplifier gain
K_{vco}	Hz/volt	Loop oscillator constant
K_x	Hz/Hz	Frequency multiplier multiplication factor
a	--	Limiter suppression factor at loop threshold
G_o	1/sec.	Threshold loop gain ($2 \quad K_m K_a K_{vco} K_x$)
$\theta_i(s)$	rad	Phase input to loop
$\theta_o(s)$	rad	Phase output to loop (phase of loop oscillator)
$F_1(s)$	--	Loop filter transfer function
T_1	sec.	Loop time constant ($T_1 = R_1C$)
T_2	sec.	Loop time constant ($T_1 = R_2C$)
B_o	rad/sec.	Loop natural resonant frequency
$H_o(s)$	--	Open loop transfer function
H(s)	--	Closed loop transfer function
2BLO	Hz	Loop two-sided noise bandwidth at threshold

The solution to this contour integral numerically expresses the loop natural resonant frequency in terms of the two-sided loop noise bandwidth as shown by equation 8.

$$2\,BLO_{Hz} = 1.06\,B_o \text{ rad/sec.} \tag{8}$$

The loop design was correlated with laboratory simulation*, test results and the link analysis. The C/N_o was taken to be 43 dB. If 5-dB carrier suppression due to modulation is allowed, the C/N_o available to the carrier track loop is 38 dB. Laboratory simulation test data revealed that the signal-to-noise ratio in the carrier track loop must be +15 dB to prevent thresholding of the demodulated baseband. If gaussian noise is assumed, it follows that with a C/N_o of 38 dB the two-sided loop noise bandwidth must be 200 Hz to maintain a signal-to-noise ratio of +15 dB. Further, the loop natural resonant frequency becomes 212 rad/sec. as defined by equation (8). Figure 2.3 is a block diagram of the tracking unit which will aid in following the discussion below.

*This simulation was performed during the design plan phase of the contract to verify analytical results.

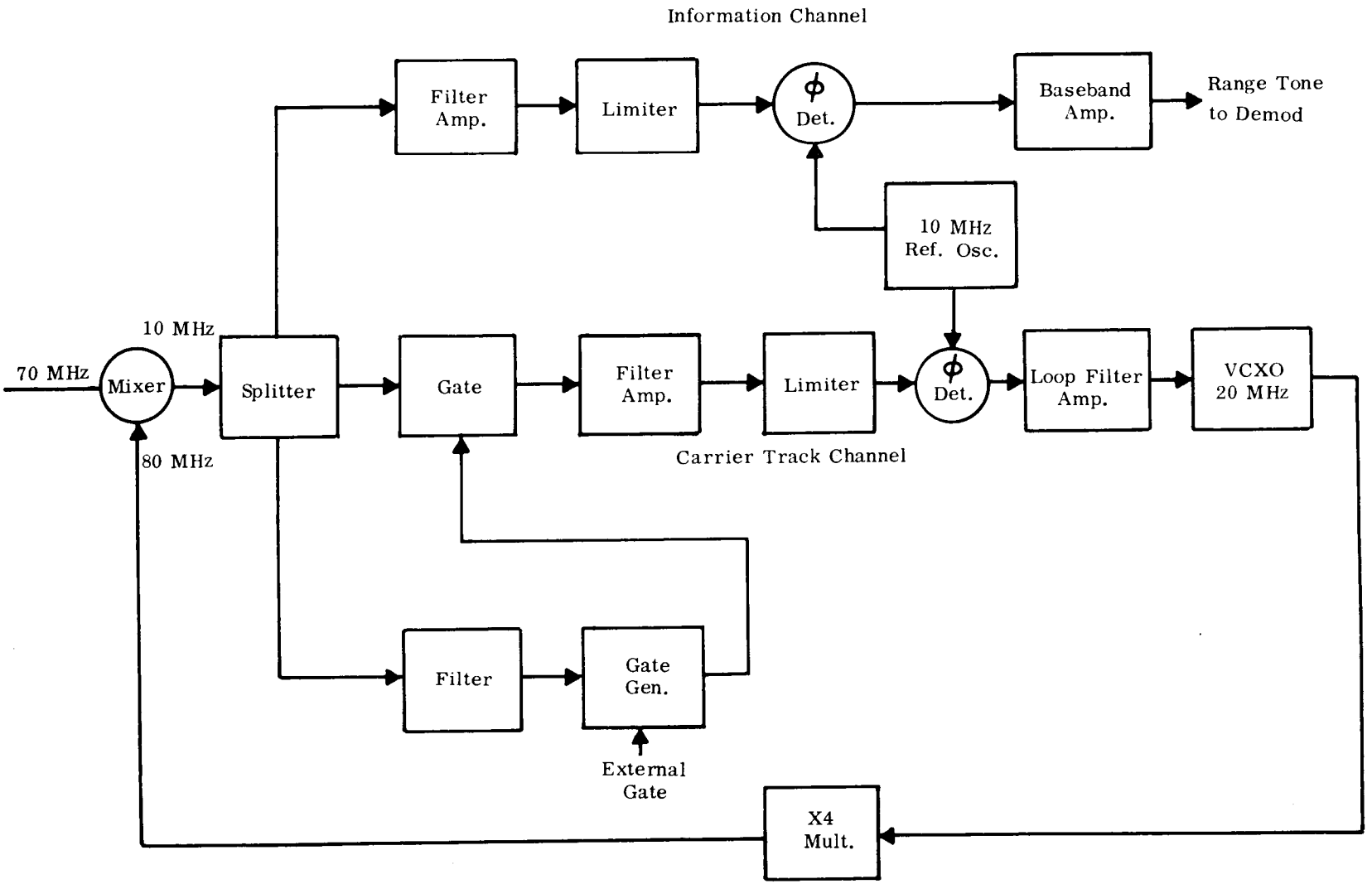

Figure 2.3 Simplified Carrier Tracking Unit Block Diagram

The simulation indicated that the loop pull-in time is greatly enhanced if the VCO frequency established at the trailing edge of one burst is "held" by a sample/hold unit inside the loop or alternatively by making the loop filter time constant, T_1, long compared to the time between bursts. The time between bursts is approximately 760 Ms. If T_1 is 7.6 sec. to satisfy the "hold" requirement, then the open-loop gain becomes 110 dB as defined by equation (3). This is a realistic open-loop gain and this approach does not require a sample/hold circuit. This loop gain will result in only about 3 degrees of phase error when the system is stressed with maximum doppler frequency shift (3 kHz) attributed to aircraft motion.

The gain contribution of each loop component as indicated by equation (1) is designed to yield an open-loop gain of 110 dB (at loop threshold). As shown by equation (1), the open-loop gain is diminished by the Limiter Suppression** factor, α. The limiter suppression is determined by the signal-to-noise ratio in the predetection bandwidth. As stated earlier, the two-sided loop noise bandwidth is 200 Hz. The predetection crystal filter noise bandwidth is 2000 Hz. At loop threshold the signal-to-noise ratio in the loop two-sided noiseband is 0 dB (by definition). Therefore, in the predetection noise bandwidth the signal-to-noise ratio will be -10 dB. The limiter suppression (σ) for -10 dB signal-to-noise ratio is 0.3, or -10 dB. Therefore, the open-loop gain must be 120 dB on a strong signal (at the center of the burst) and the open-loop gain will degrade to 110 dB at loop threshold.

2.1.3 Gating

The carrier track loop was designed to be gated by the spin scan synchronizer in synchronism with the spin of ATS-5. This synchronizer, which was used on previous ATS experiments, was located at Mojave. A receiver gate circuit was installed (figure 2.3) in the 10-MHz carrier track loop IF which permitted gating the signal through the loop only when the spacecraft was illuminating the ground station. This prevented system noise from driving the voltage controlled crystal oscillator (VCXO) off frequency when no spacecraft signal was available. To permit more flexibility in using the equipment, this circuit was modified in the field to also permit self-gating by using the receive signal level to develop the gate pulse.

2.1.4 Range Demodulator

A baseband signal is produced in the carrier track receiver which contains either 4-kHz or 20-kHz range tone information. The signal is periodic in nature, having an amplitude variation frequency which corresponds to the ATS-5 spin.

** See Glossary

The range demodulator receives this signal which has a signal-to-noise power density (S/N_o) in both sidebands of 48 dB. Again, as in the carrier track loop, a 3-dB design margin was used which reduces the S/N_o available to the range demodulator to 45 dB. Design of the range demodulator and in particular the digital phase lock loop was based upon this signal-to-noise ratio and a measurement accuracy goal in the order of 100 feet (approximately 100 nanoseconds).

The baseband signal containing range information is filtered and hard limited and then applied to the phase detector of a digital phase-lock loop. The purpose of the loop is to synthesize the received signal with a high degree of resolution over many cycles of the range tone signal during each signal burst from the spacecraft. The synthesized signal is then phase compared to a stable reference signal to provide a measure of the phase delay which results from the transmission path.

A complete anslysis of the range demodulator requires rather extensive mathematical manipulation. For this reason, only a summary analysis is given in this section. A much more rigorous analysis of this unit is provided in Appendix A and the addendums.

2.1.4.1 Analog Filters

The analog filters serve two purposes: they reduce the aliasing* effects of the digital phase lock loop and they increase the signal-to-noise power ratio in the limiters.

The input signal-to-noise (S/N_o) will be greater than 45 dB-Hz. A filter bandwidth of 16 kHz will provide an output S/N greater than 3 dB. This is a reasonable minimum value to use into the limiters.

A second-order maximally flat bandpass response was selected. The denominator polynomial of the low-pass maximally flat Butterworth response is given as:

$$S^2 + \sqrt{2}\,S + 1 \qquad (1)$$

With a 16-kHz bandwidth and a 20-kHz center frequency, the elementary low-pass to bandpass transformation replaces "S" by:

$$S \Rightarrow 5/4\,(S + 1/S) \qquad (2)$$

The response then is:

$$G(S) \cong \frac{6.4\,\omega_o^2\,S^2}{(S^2 + 0.406\,\omega_o\,S + 0.56\,\omega_o^2)(S^2 + 0.725\,\omega_o\,S + 1.785\,\omega_o^2)} \qquad (3)$$

*See Glossary

where $\omega_o = (2\pi) \times 4 \times 10^3$ for the 4-kHz tone

and $\omega_o = (2\pi) \times 2 \times 10^4$ for the 20-kHz tone

The input signal level is -3 dBm. The limiters are able to handle input levels 20 dB above this. Therefore, an additional 20-dB gain for the filter was specified.

2.1.4.2 Phase-Lock Loop

Functional elements of the phase-lock loop are; phase detector, phase shifter, phase shifter control, and divide-by-N circuit. The gain for the phase-lock loops, and the accuracy of each update is determined within the phase detector.

The function of the phase detector is to measure the phase difference between the tone recovered from the baseband and the phase locked tone, and provide correction signals for the phase-lock loop.

The only important contribution to measurement uncertainties in the phase-lock loop is the input signal-to-noise ratio. For 4-kHz ranging, which is used only to resolve the 50- μ sec. ambiguities in the 20-kHz range readings, a 45-dB Hz baseband signal (tone)-to-noise ratio produces a range uncertainty with standard deviation of about 718 nsec. For 20-kHz tone ranging the 45 dB-Hz signal-to-noise ratio results in a range uncertainty of about 105 nsec.

The quantization is 20 nsec. which introduces an error with standard deviation of: $\langle \Delta^2 \rangle$ denotes expected value of Δ^2

$$\langle \Delta^2 \rangle^{1/2} = \sqrt{\frac{20}{12}} \cong 5.8 \text{ nsec.} \tag{4}$$

The error due to phase uncertainties of the prefilter has a standard deviation claculated to be less than 125 nsec. for 4 -kHz tone ranging and less than 25 nsec. for 20-kHz tone ranging.

The overall range uncertainties due to all three sources are:

$$\sigma = \sqrt{(718)^2 + (5.8)^2 + (125)^2} \tag{5}$$

or

$$\sigma \cong 730 \text{ nsec. for 4-kHz tone}$$

and

$$\sigma = \sqrt{(105)^2 + (5.8)^2 + (25)^2} \tag{6}$$

or

$$\sigma \cong 117 \text{ nsec for 20-kHz tone}$$

The signal used to synthesize a range tone is received in periodic bursts due to the spinning of the ATS-5 spacecraft. The best range information occurs near the end of each burst, at which time the reading is punched on paper tape and the range display is updated. Thus, the detection and display/punch-out is cycled at the satellite spin period - about 790 msec.

Each phase detection cycle is initiated by the "RF DET GATE" from logic board A2B (figure 2.4). The "RF DET GATE" is enabled by the "REC GATE" from the spin scan synchronizer or internal gate circuit which is delayed to allow transients in the carrier track and prefilter to settle out. The period of the "RF DET GATE" is 40 msec., which is sufficient time for 160 cycles of 4 kHz, or 800 cycles of 20 kHz. An "UPDATE GATE" (A1E) is generated at the end of each cycle of the received signal and is terminated by the phase-locked signal. If the received signal leads the phase-locked signal, the direction of the update is up, and vice versa. The magnitude of the update is a function of the phase error between the received and phase-locked signals, measured in 20-nsec. increments utilizing a 50-MHz clock and the gain of the phase detector.

At the end of the update period, the control counter and the phase shift counter are simultaneously enabled. The phase shift counter begins to count up or count down until the control counter becomes saturated and disables the phase shifter counter. During the enable period, the BCD count from the phase shift counter is converted to decimal and used to gate out one of ten 5-MHz signals. These 5-MHz signals are spaced in 20-nsec intervals. The 5-MHz signal is divided by either 250 or 1250 to generate the 20-kHz phase-locked signal or the 4-kHz phase-locked signal, respectively.

2.1.4.3 Range Resolving Logic

The function of the range resolving logic is to measure the phase difference between the reference signal and the phase-locked signal and to resolve this difference into a range measurement.

After the 40-msec. "RF DET GATE," the range gate generator is enabled. The reference signal, which is shifted to negate any delays in the system, is utilized to start the "RNG GATE" and the phase-locked signal is utilized to end it. The duration of the range gate is proportional to the range as a function of time.

The range measurement from the range register will be read out on a visual display and simultaneously will be multiplexed along with the time of day to be punched out on paper tape.

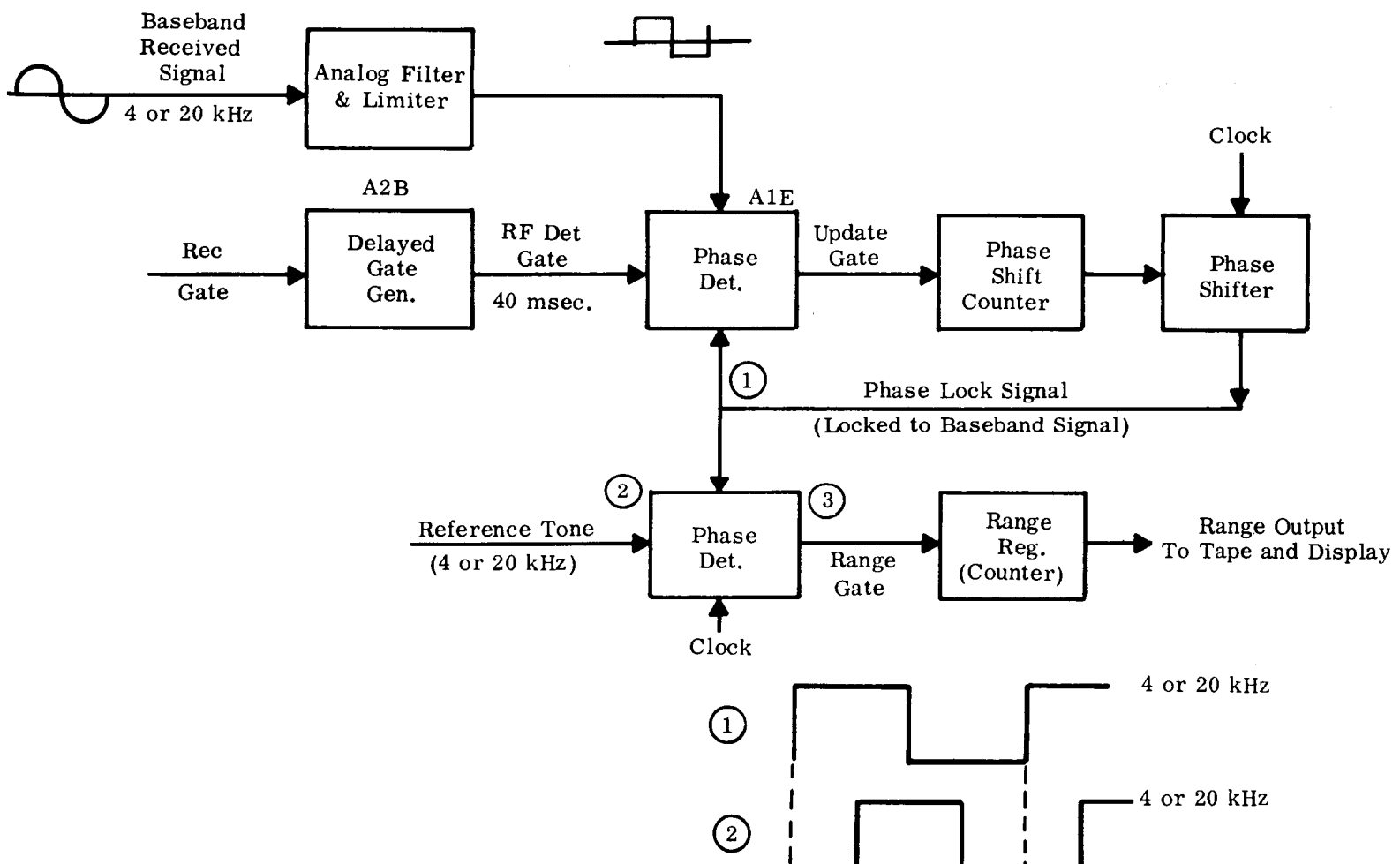

Figure 2.4 Simplied Range Demodulator Block Diagram

2.2 RANGING RECEIVER

The ranging equipment designed and fabricated on the ATS-5 L-Band Ranging and Position Location contract is housed in a standard 19-inch equipment rack. The system, illustrated in figure 2.5, is 6 feet high by 24 inches in depth. Since it is a special experimental unit, it was designed for ready mobility and may be easily set up in a variety of test configurations.

The equipment as shown in figure 2.5 consists of:

Carrier Tracking Unit
Range Demodulator
Paper Tape Punch
Patching and Interconnection Panels
Power Supplies

The system was designed to interface a radio receiver down-converter at an intermediate frequency of 70 MHz, and to carrier-track a pulse-type signal that has been angle modulated with ranging tones. The range information is extracted from the tone in the range demodulator unit, digitized, and recorded by the paper tape punch unit in an eight-level code* format. The performance characteristics are listed in Table 2.3.

2.2.1 Carrier Tracking Unit

A block diagram of the carrier tracking unit is given in figure 2.6. The unit phase-locks to a 70-MHz carrier input, and supplies a demodulated baseband output signal to the ranging demodulator. The unit will track the 70-MHz input carrier over a range of at least ± 2.5 kHz. The input impedance is 50 ohms, and a 70-MHz carrier level of at least 0 dBm is required for optimum performance. An amplifier capable of 12-dB gain and with an input/output impedance transformation of 75/50 ohms is provided for use with radio down-converters having lower output levels and different output impedances. A 70-MHz signal splitter is also provided to facilitate front panel monitoring of the carrier tracking unit input signals.

The second output from the splitter is mixed with a nominal 80-MHz signal to produce a carrier tracked difference frequency of 10 MHz. The 10-MHz output from the mixer (A25) is split three ways by splitter A29. One output port is connected to a 10-MHz filter whose bandwidth is 3 kHz at the 3-dB points. The output of this filter is used to generate a gating signal synchronous to the spin of the ATS-5 satellite. The bandwidth restriction of the filter is utilized to provide maximum level

*See Glossary

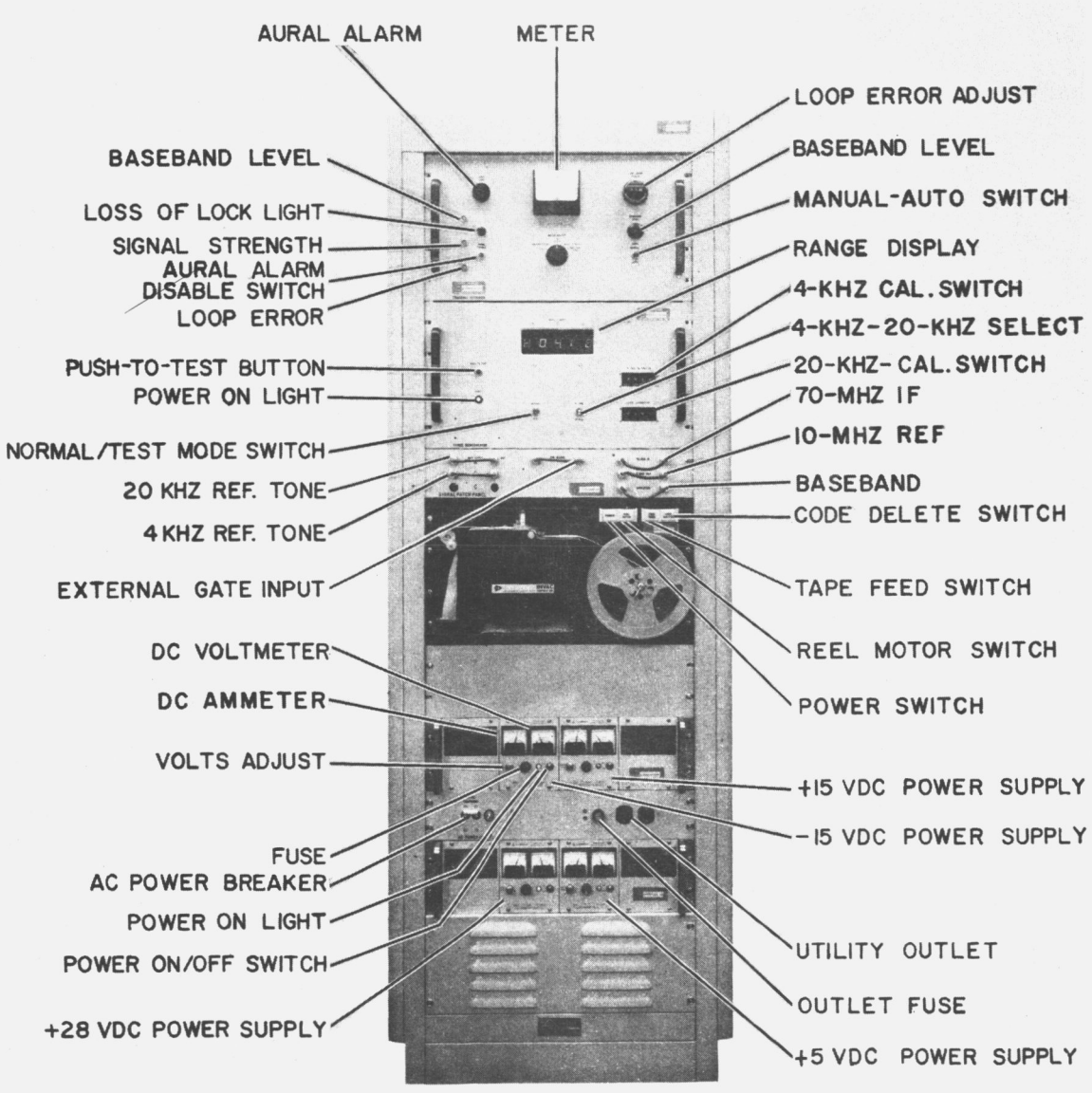

Figure 2.5 Rack Layout of Ranging Equipment

TABLE 2.3 RANGING RECEIVER CHARACTERISTICS

Ranging Receiver	
Input Level	-3 dBm nominal
Input Impedance	75 ohms
Input Frequency	70 MHz
Modulation	Angle mod to 1.5 rad peak
Reference Tone Frequency	4 or 20 kHz
Reference Tone Level	-3 to +10 dBm
Ranging Accuracy	Better than 100 ft. RMS for 51 dB C/N_o
Max. lock-up time (20 kHz)	26 secs. (to within 100 nsec. error)
(20 kHz)	37 secs. (to within 20 nsec. error)
Time of Day Input	BCD-hours, minutes, seconds 0 to -6 V (with -6V = logical 1)
Range Output (visual)	4 decimal digits
(tape)	5 decimal digits
Temperature Range	
(operating)	0^{o} to 40^{o} C
(non-operating)	0^{o} to 65^{o} C
Altitude (operating)	6000 feet
(non-operating)	50,000 feet
Carrier Tracking Unit	
Input Level	+5 dBm nominal
Imput Impedance	50 ohms
Input Frequency	70 MHz
Information Channel BW	300 kHz
Tracking Channel BW	5 kHz
Pull-in Range	$\pm$1 kHz
Hold-in Range	$\pm$3 kHz
Baseband Output BW	100 kHz
Baseband Level Output	0 to +10 dBm

TABLE 2.3 RANGING RECEIVER CHARACTERISTICS (Continued)

Range Demodulator

Input Frequency	4 or 20 kHz
Input Level	-3 to +10 dBm
Clock Frequency Input	10 MHz
Clock Level	+13 dBm nominal
Processing BW	10 Hz
Data Output	Tone code plus 4 digits of time delay in microseconds.

Tape Punch

Input Levels (0, 1)	0 V and +4V nominal
Data Code	8-level ASCII*
Data Format	

Character	Function	Units
1	Start	Line Feed
2	TOD (6 digits)	10 hr.
3		1 hr
4		10 min.
5		1 min.
6		10 sec.
7		1 sec.
8	Tone Code	H or L
9	Data (5 digits)	100 usec.
10		10 usec.
11		1 usec.
12		100 nsec.
13		10 nsec.
14	Stop	Carriage Return

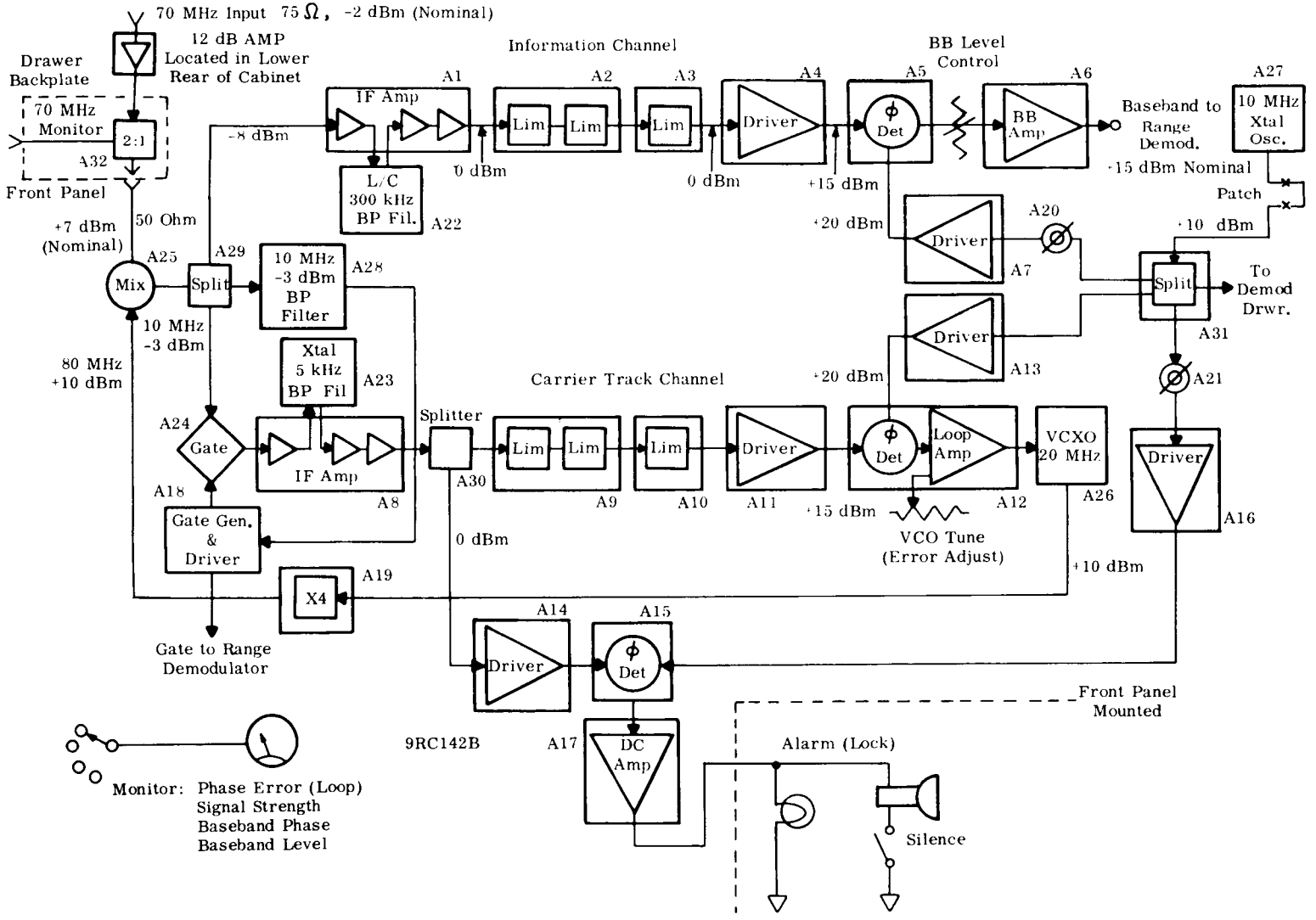

Figure 2.6 Carrier Tracking Unit Block Diagram

differential between the 70-MHz carrier and the noise. A level detector in the gate generator (A18) is set to reject the side lobes of the spinning satellite antenna pattern. The level detector responds to the carrier power of the main antenna lobe, and thus a gate signal is generated in synchronism with the spin of the satellite. Under normal received carrier level conditions, this gating signal has a duration of about 100 to 120 milliseconds.

The second port of splitter A29 is fed to the gated carrier tracking channel. The IF amplifier of this channel is held to a 5-kHz bandwidth by crystal filter A23. The filter passband was selected to reject the ranging tone modulation sidebands at $\pm$4 kHz (or greater) fromthe carrier. This rejection is necessary to ensure that the receiver will lock-up on the desired 10-MHz carrier rather than one of its tone modulation sidebands.

The amplified carrier is next divided by splitter A30. One port of the splitter is fed to a "loss-of-lock" alarm circuit where the incoming carrier is phase compared to the receiver standard, A27. If the received carrier is not in phase with the standard 10-MHz oscillator (A27), the alarm circuitry will be energized. The alarm circuitry has a 10-second dropout delay to inhibit false alarm activation during the time period when the satellite antenna is not oriented towards Earth. The second port from splitter A30 drives the limiter section of the carrier track channel. These limiters and the driver (A9, A10, and A11) are identical with those of the main information channel (A2, A3, and A4). The limiters are designed for minimum differential phase shift as a function of the degree of limiting. Thus the phase-lock loop parameters are largely determined by the crystal filter, A23, and the loop amplifier, A12.

The narrow bandwidth and level-limited carrier signal is now amplified at least 15 dB by the driver A11. The phase detector compares this signal to the 10-MHz signal of the system standard, A27. The detector output is a DC voltage which varies proportionally to the phase error between the two 10-MHz inputs. The loop amplifier supplies the gain required to control the frequency of the 20-MHz VCXO, A26. This nominal 20-MHz signal is multiplied four times and filtered by A19 to produce the controlled 80-MHz input for mixer A25. The 10-MHz output of A27 is fed through a front panel patching connection which facilitates use of an external clock if necessary or desired.

The information channel receives its 10-MHz input from a third output port of splitter A29. The IF amplifier and driver for this channel is nearly identical to that of the carrier track channel. The bandpass filter (A22) provides an information channel bandwidth of 300 kHz. This relatively wide passband is required to allow the carrier plus its modulation sidebands to be passed through the circuitry. The wide bandwidth is also useful in that it permits use of modulation other than the 4-kHz or 20-kHz range tones. The 10-MHz comparison input to the phase detector, A5, is passed through a phase shifter network, A20. This shift is incorporated to correct for the phase delay introduced by the tracking loop. This delay is introduced via the 80-MHz input to mixer A25. The baseband output from A5 is fed through the baseband level control to the baseband amplifier, A6, to bring the recovered range tone up to the level required for nominal operation of the range demodulator (+15 dBm).

2.2.2 Range Demodulator

A simplified block diagram of the range demodulator is given in figure 2.7. This unit accepts the baseband signal and gate signal from the carrier tracking unit; uses the gate signal for timing purposes; compares the baseband tone (4 or 20 kHz) to the reference tone; and thus determines the measured range in terms of nanoseconds of difference between the received and transmitted (reference) range tones. The measurement is ambiguous in that the number of integral cycles of delay is not known at this point. The ambiguity is resolved during the processing of the recorded data.

The range demodulation process is turned "ON" by the gate signal from the carrier tracking unit via unit A2B. This gate is present at the range demodulator interface (A2A) for about 120 milliseconds during each revolution of the ATS-5. The interface circuit (A2A) delays the gate signal approximately 40 milliseconds. The gate signal is then applied to A1E, where the receiver baseband signal is phase compared to a locally generated ranging tone.

The locally generated tone is derived from the 10-MHz input from the system clock (A27 in the carrier tracking unit drawer). The clock input is amplified and converted to 25 MHz by units A7A, A7B, and A7C as shown in figure 2.7. Unit A1A generates a 5-MHz clock which is divided into 10 separate signals in the phase shifter, A1C. Each of the 10 clock signals is delayed 20 nanoseconds so the entire 200-nanosecond time spectrum for a 5-MHz signal is divided into 10 equal parts. One of these 10 clock signals is selected by unit A1D, and divided in A1G by a number "N" such that the output is either 4 kHz or 20 kHz.

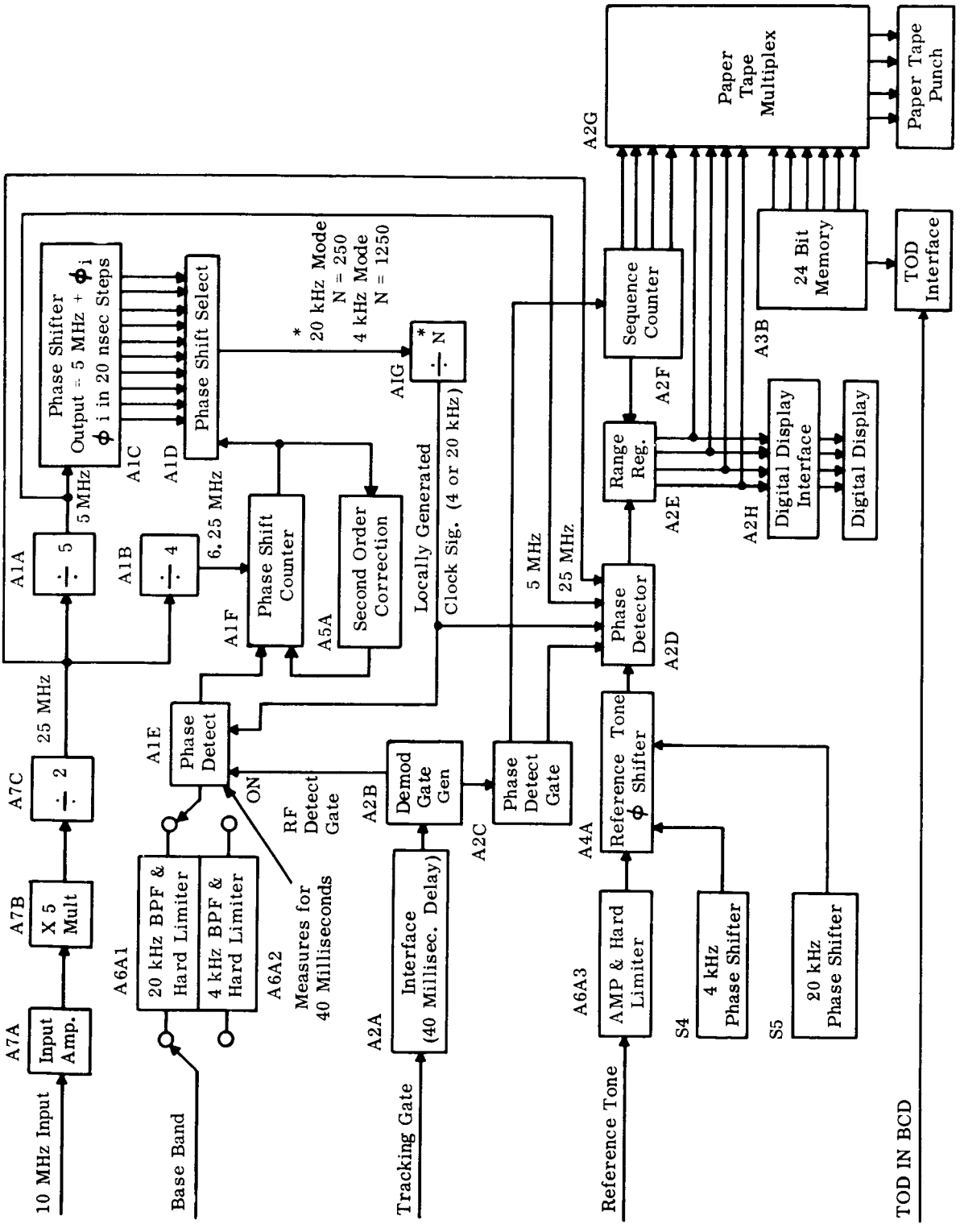

Figure 2.7 Range Demodulator Block Diagram

The baseband signal from the carrier tracking unit is filtered and hard limited in A6A1 or A6A2. This square-wave signal is then phase compared to the locally generated clock by phase detector, A1E. The phase detector first determines whether the local clock leads or lags the baseband signal, and enables a gate to the phase shift counter (A1F) when the first of the two comparison signals is detected. The latter of the two signals acts to disable the gate and stop counter, A1F. The phase shift counter measures the time differential between the baseband input signal and the locally generated clock signal by counting the cycles of 6.25 MHz that occur between them. The phase shift select circuit, A1D, selects the necessary output from the phase shifter, A1C, to minimize the phase error detected by circuit A1E.

The above-described range measurement is carried out for a 40-millisecond time period during each satellite revolution. This means that 800 cycles of the 20-kHz range tone (or 160 cycles of the 4-kHz tone) are utilized for phase-lock purposes in in each revolution. Since the satellite (and possibly the ranging receiver) is moving, the phase differential changes with time. The correction circuit, A5A, acts to monitor this change over the 40-millisecond comparison period. The change in count over the period is accumulated by A5A and dumped into the A1F phase shift counter at the beginning of the next comparison period. The range tone obtained as a result of the above process is phase-locked to the incoming baseband signal with a maximum inherent error (due to equipment design) of $\pm$10 nanoseconds. This error is derived as a result of the minimum steps available from phase shifter A1C.

The phase-locked range signal also appears as an input to phase detector A2D. The comparison input to this detector is the reference tone. This reference tone may be the 4-kHz or 20-kHz signal from the station ATSR equipment, or it may be a tone derived from a suitable frequency standard. In any event, the reference tone must be coherent with the baseband signal applied to the A1E phase detector. The reference tone signal is amplified and hard limited by A6A3 and phase shifted in unit A4A (the reason for this phase adjustment will be discussed later). The tone signal is next applied to phase detector, A2D.

Phase detector A2D is normally in operative until a "START" signal is received from gate unit A2C. This same start signal causes the sequence counter (A2F) to reset the range register (A2E) to zero in preparation to receive the upcoming range measurement. This start signal is timed to occur at the end of the 40 milliseconds of phase comparison in unit A1E. Phase detector (A2D) then counts the

number of cycles of 5-MHz or 25-MHz clock signals that occur between the first negative-going zero crossing of the reference tone and that of the phase-locked baseband signal from A1G. The 5-MHz count is used with 4-kHz tone ranging, and the 25-MHz count is used with the 20-kHz range tone. Thus the maximum inherent equipment error is 40 nanoseconds with the 20-kHz ranging tone and 200 nanoseconds with a 4-kHz tone. This error is in addition to the maximum possible equipment error of 10 nanoseconds described above. The range count is accumulated in range register A2E. At the end of the count period, the output of the range register is fed in a four-digit parallel format to the digital display interface (A2H) and the paper tape multiplex unit (A2G).

The digital display interface unit is capable of high-speed conversion of binary coded decimal information into the proper code for driving a four-digit visual display. The display consists of four vacuum fluorescent readout tubes. The paper tape multiplexing unit performs the logic required to format the range data for proper output to the paper tape punch. A second series of parallel inputs to the multiplexer is the time-of-day (TOD) information obtained from the station clock. TOD is interfaced into a 24-bit memory. When the sequence counter initiates the printout function, the TOD is transferred from the memory unit and formatted in the muliplexer for the punch unit. The next unit of information to be transferred to the punch is a code to designate whether the machine is in the 4-kHz or 20-kHz mode of operation. Next, the range reading is formatted and sent to the punch unit, followed by an end character that completes the output sequence. The completion of the output sequence completes one pass through the ranging demodulator. On the next pulse from the receiver gate, the demodulator sequence is initiated again.

As mentioned previously, the reference tone is phase-shifted prior to phase detection. The reference tone (either 4-kHz or 20-kHz) from the ATSR or frequency standard is amplified and hard limited to produce a clean square wave. This signal is then applied to a reference tone phase shifter, A4A. This phase shifter compensates for any phase delay introduced by the system hardware. The required phase shift compensation is manually introduced into the phase shifter by two panel-mounted, four-decade thumbwheel switches (one set for each mode of operation). To set in the proper phase shift, it is necessary to range to some known location, such as the collimation tower, and adjust the thumbwheel switches until the proper range readout is obtained at the digital display unit.

2.2.3 Digitronics Model 1560 Paper Tape Punch

This paper tape punch is a solenoid-actuated tape perforator with associated electronics capable of punching 5-, 6-, 7-, or 8-channel paper tape. The punch will operate at a rate up to 60 characters per second. The mechanical unit consists of nine tape punch mechanisms (one for each of the eight data channels and one sprocket channel) and a tape transport mechanism. The electronics of the unit consists of a regulated power supply and the interfacing logic. The punch unit receives the multiplexed data from the demodulator and outputs this in a serial manner on eight-channel paper tape. The entire unit is housed in one drawer of the ranging equipment assembly (figure 2.5).

2.2.4 Lambda Regulated Power Supplies

These power supplies (there are four separate units) provide +5V, ±15V, and +28V for the entire cabinet. They are basically full-wave rectifiers, provided with capactive filtering, and incorporating series regulation in the output circuitry. The four power supplies are housed in two drawers of the ranging equipment rack. Each unit is self-contained and incorporates its own voltage and current metering, overload protection, and main power switch.

2.2.5 Patching and Interconnection Panels

The rack contains two separate patch panels. One panel was installed during the fabrication of the equipment, and the other was installed in the field as more equipment interfaces became necessary. The main patch panel contains jumper cables for the reference tones, 10-MHz clock, 70-MHz signal, and the baseband signal. It also contains a switch for selecting the spin gate (either an internal one pulse per second, or a gate derived from the ATS-5 signal). The panel also provides a monitor point for the spin gate signal. The unit has been drilled to accept up to three reference tones if necessary. The smaller of the two patch panels contains three interface connections between the strip chart recorder and the receiver. It also contains a 70-MHz test point and a received signal strength test point.

SECTION 3

FIELD INTEGRATION

3.1 EQUIPMENT CONFIGURATION

The L-band ranging receiver arrived at the Mojave STADAN station 15 January 1971 and was immediately installed in accordance with the preliminary Installation Control Directive (ICD) dated 4 January 1971. During the following equipment checkout and acceptance testing phase the interface configuration was changed to improve performance and simplify the experimental testing effort. These changes were incorporated into the ICD and supplied to the ATS project group at GSFC. The final interface configuration is shown in figure 3.1 Details of various changes are provided in the following paragraphs.

3.2 INSTALLATION MODIFICATIONS

3.2.1 70-MHz Interface Modification

The ranging receiver was designed to provide optimum performance with an input signal level of +5 dBm. An examination of the available 70-MHz signal level at the ranging receiver input showed this level to be approximately -2 dBm. An amplifier, which was surplus from a previous L-band experiment, was modified to provide 12 dB of gain at 70 MHz. The input impedance of the amplifier was 70 ohms and the output impedance was set at 50 ohms to match the carrier track unit impedance. This eliminated the need for the 70/50 ohm matching circuit originally incorporated in the equipment design.

A 2:1 power divider was added following the 12-dB amplifier to provide 70-MHz outputs, each at +5 to +7 dBm nominal. One output serves as the carrier track unit input, while the other is brought out to the front panel to provide a 70-MHz signal monitor point.

3.2.2 20-kHz Modification

The 20-kHz reference tone which is taken from the ATSR ranging equipment was found to be only 0.3 V, whereas the ranging receiver requires 0.5 V for normal operation. To raise this signal to an acceptable level an HP 461 amplifier and an attenuator were added. These provided a minimum of 1.5 V at the reference tone input to the ranging receiver.

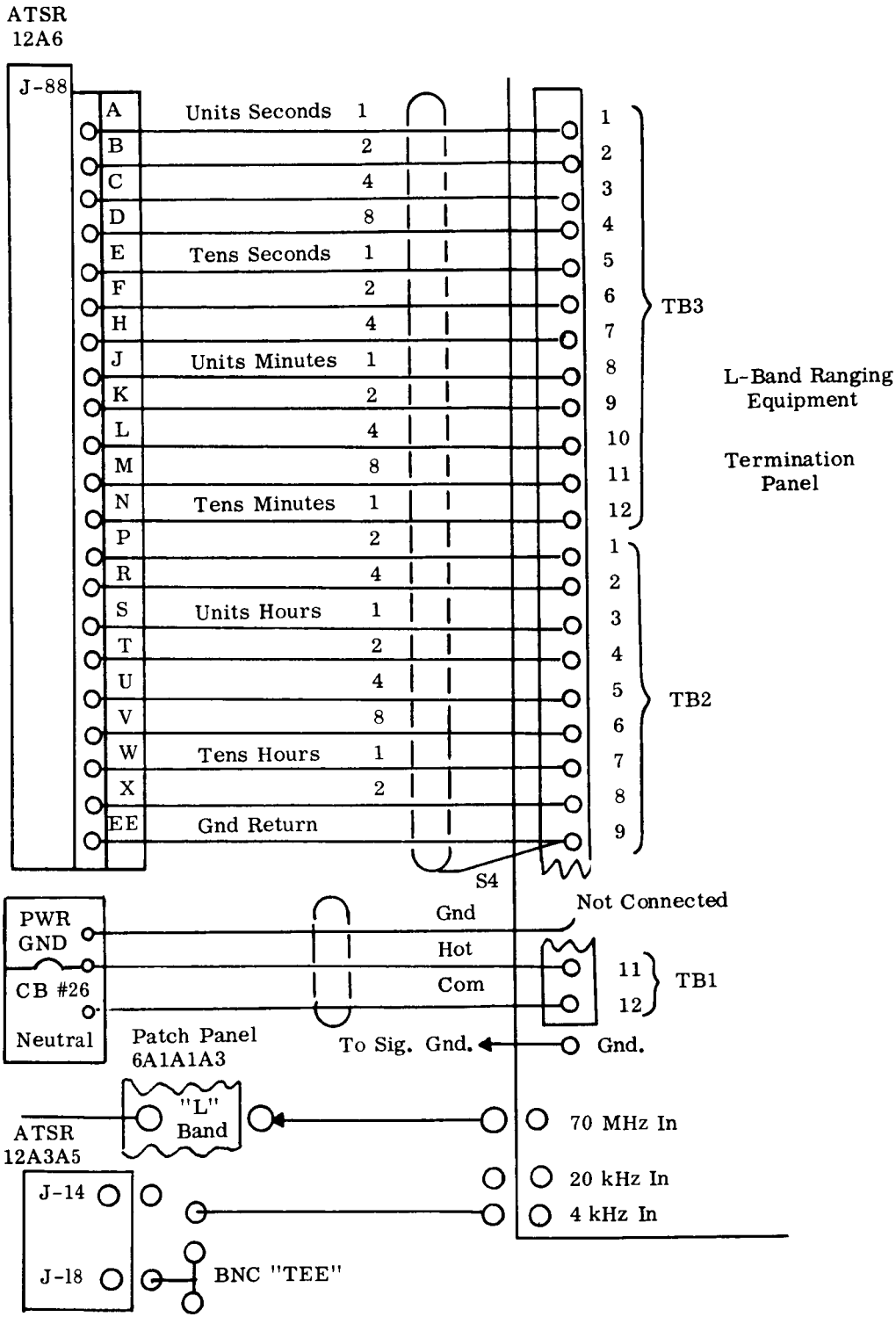

Figure 3.1 L-Band Ranging Receiver Interface

3.2.3 Grounding Modification

To conform to station grounding requirements a ground bus was installed within the ranging receiver cabinet.

3.2.4 Gating Modifications

The ranging receiver was originally designed to use the spin scan synchronizer to gate the ranging receiver in synchronism with the spin of ATS-5. Under test conditions it proved to be inconvenient to use this configuration. To circumvent this situation a gating circuit (detailed below) was added. This circuit gated on the received signal and did not necessitate using the spin scan synchronizer. The spin scan input was not removed, however. A switch was also added to permit switching from the new gating circuit in the operational mode to an internally generated 0.5 PPS gate for testing and for use with CW signals.

The circuit shown in figure 3.2 was added to provide gating from the spacecraft signal. This circuit takes a sample from the 10-MHz phase locked loop IF, filters it (3-kHz bandwidth), and adds amplification and detection to produce an output proportional to carrier level. This level is compared to an adjustable reference level in a differential detector. When the received level exceeds the reference level, the differential detector is turned on. The resulting pulse, centered about the peak of the received signal, is adjusted in width by varying the reference voltage (turn on/turn off point). The voltage level is set to discriminate against the side-lobe signals of the revolving satellite antenna by adjusting the "turn on" point high enough so that only the main-lobe signal level will actuate the differential detector output. The pulse feeds a driver circuit, which in turn supplies a control pulse for the carrier track unit and range demodulator.

3.2.5 Mechanical Modifications

Several mechanical changes were made to improve the equipment installation:

1. A shelf was added above the tape punch to act as a guide for cables attached to the carrier track unit.
2. Cables were spiral wrapped for more uniform conformance to drawer movement when drawers are opened.
3. A dual outlet box was mounted in place of a single outlet box inside of the rack so that power could be applied to a HP 461 amplifier mounted inside the rack.

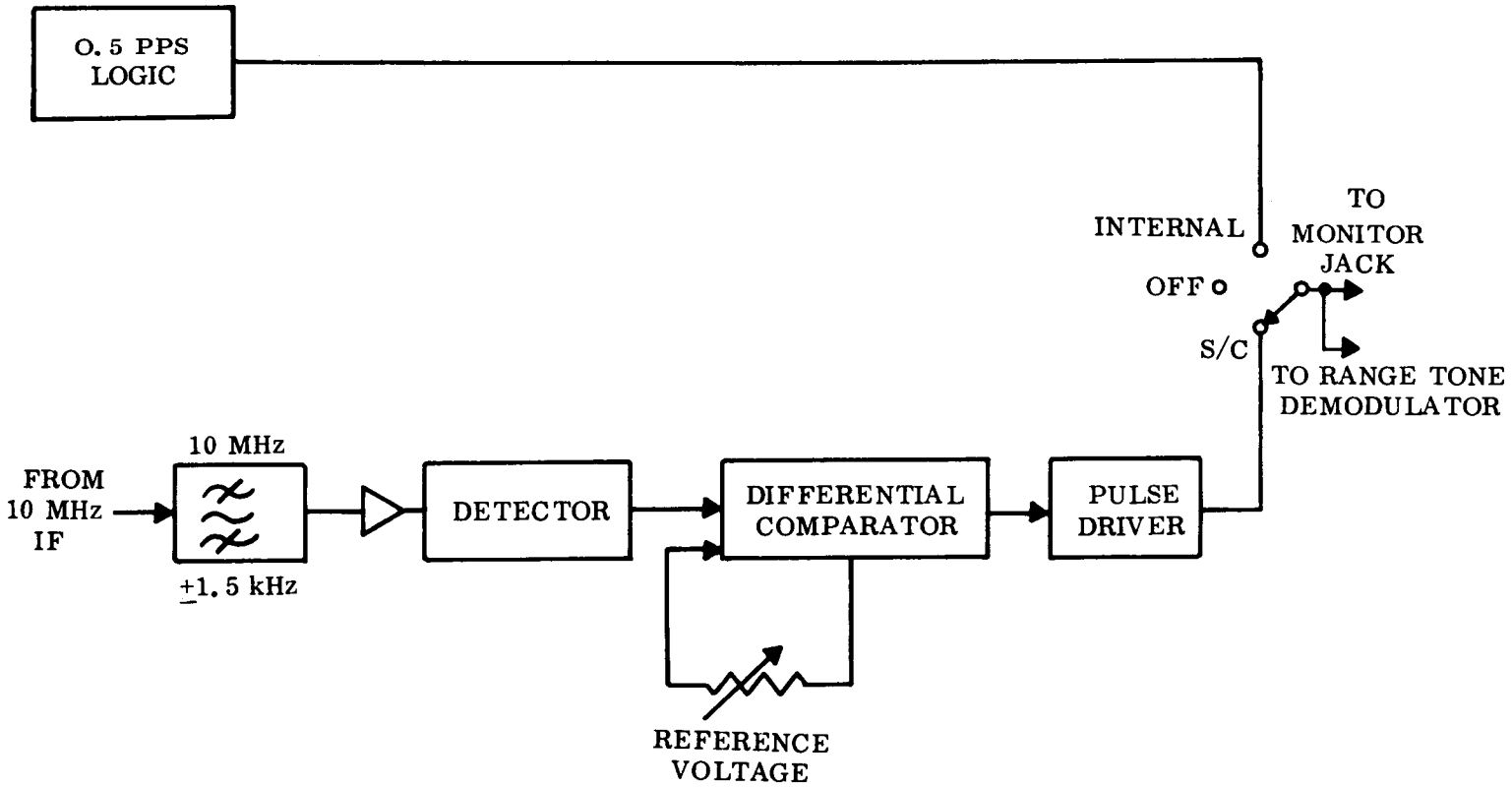

Figure 3.2 Gating Configuration

3.3 EXPERIMENT TEST RESULTS

Following equipment installation and checkout at Mojave, two variations of ranging experimentation were initiated:

(a) Ranging on ATS-5 via simultaneous C-band and L-band

(b) Position location determination via ATS-1 (C-band) and ATS-5 (L-band)

The first experiment compares ranging measurements at each frequency band against the predicted range obtained from the Goddard Orbit Determination Program. The second experiment indicates position location capabilities utilizing two satellites and a knowledge of altitude at the measuring point. L-band ranging data was collected on an eight-level punched paper tape as described elsewhere in this report. The C-band data was punched into a five-level tape by the ATSR equipment installed at each of the ATS stations. The paper tapes were returned to Westinghouse at Baltimore for processing. A computer processing program was developed which includes several calculations and methods of data presentation. The details of this program and the data derived therefrom will be presented in another report. However, typical ranging data results for each of the above two experiments are presented below.

3.3.1 Simultaneous Ranging on ATS-5

Data for this experiment was collected for several different ground L-band transmitter power levels to determine the effects of degraded signal-to-noise ratios on the L-band ranging accuracy. Each test run was conducted for a 3-minute period to obtain sufficient data points to ensure a good analysis. Table 3.1 summarizes the data obtained on one test day (25 March 1971). The range distances shown in the table are for the starting time of each test period. Detail plots for two of the ranging tests made on this day are shown in figures 3.3 to 3.6, inclusive. The slope of the graphs is caused by the movement of the satellite during the test period. The plots of figures 3.3 and 3.5 show the raw experimental data with the L-band points "corrected" for lane ambiguity by comparison to the C-band measurement. The latter figure illustrates the effect of degraded S/N ratio on the data as received and processed by the ranging receiver and demodulator. The "Smoothed Range" curves of figures 3.4 and 3.6 were obtained by fitting raw data to a second-degree polynominal using the method of least squares. This program also computes the standard deviation as shown on the curves and in Table 3.1. The other numbers shown on the graphs are

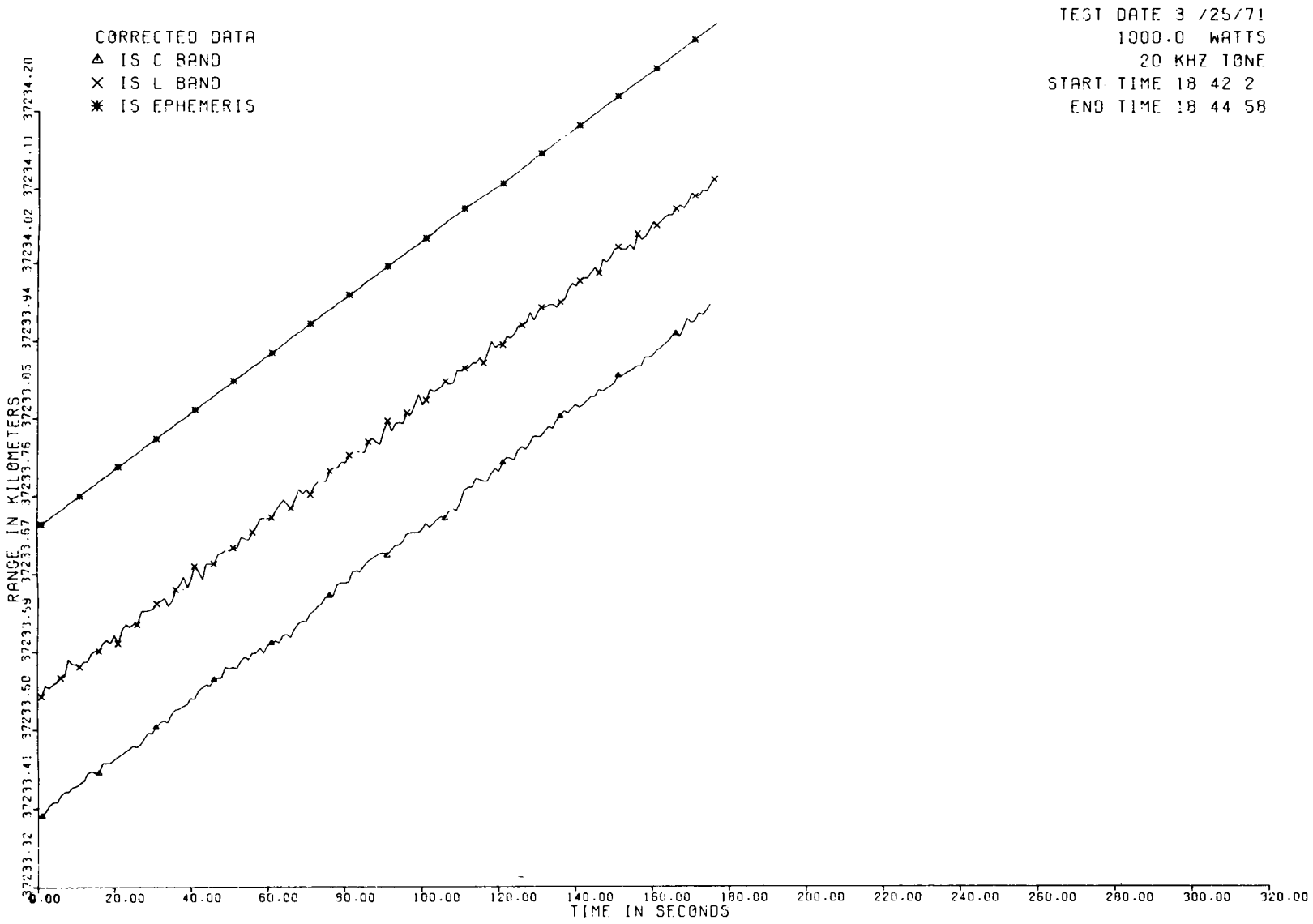

Figure 3.3 Detailed Ranging Plots, Corrected Data

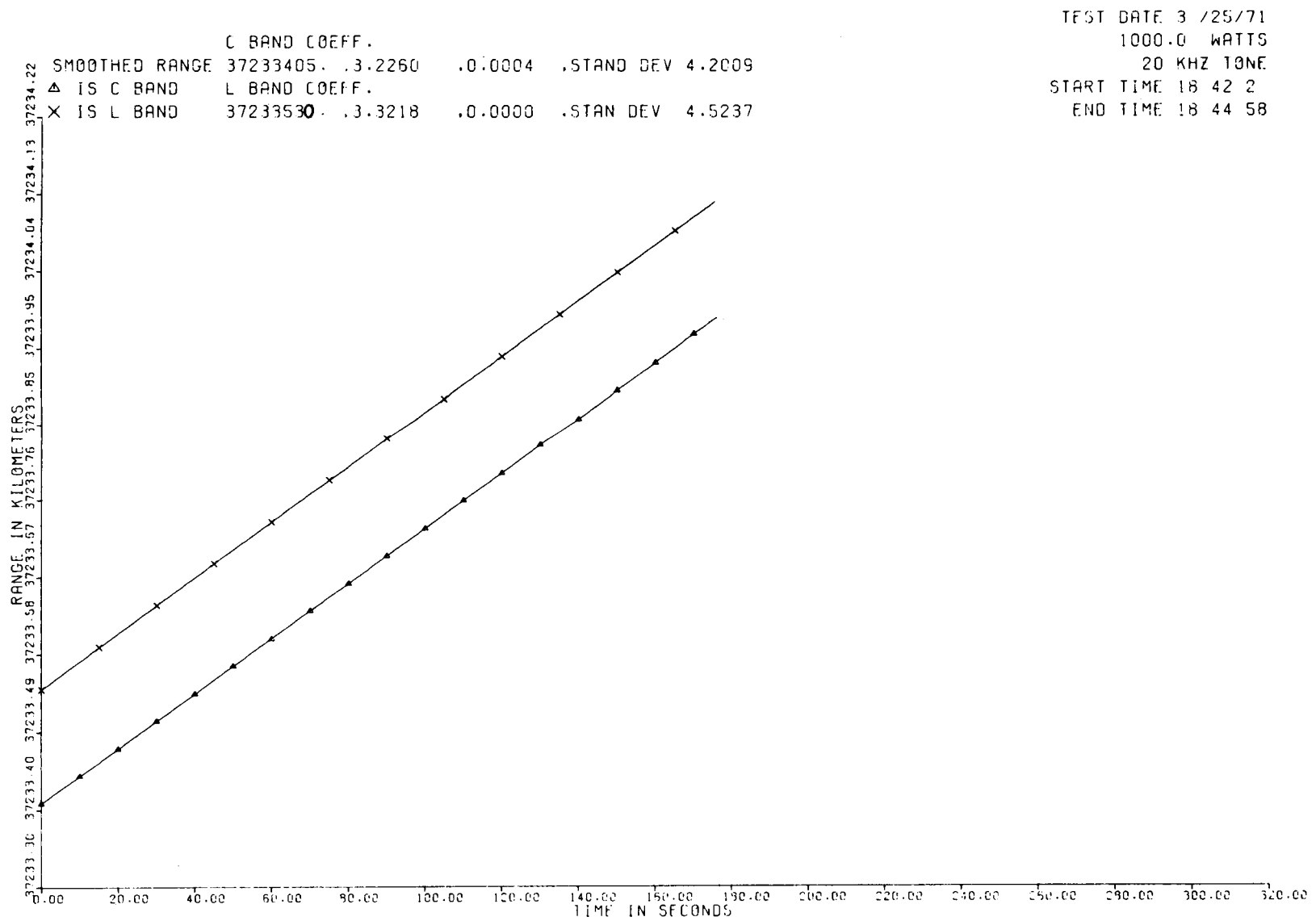

Figure 3.4 Detailed Ranging Plots, Smoothed Range

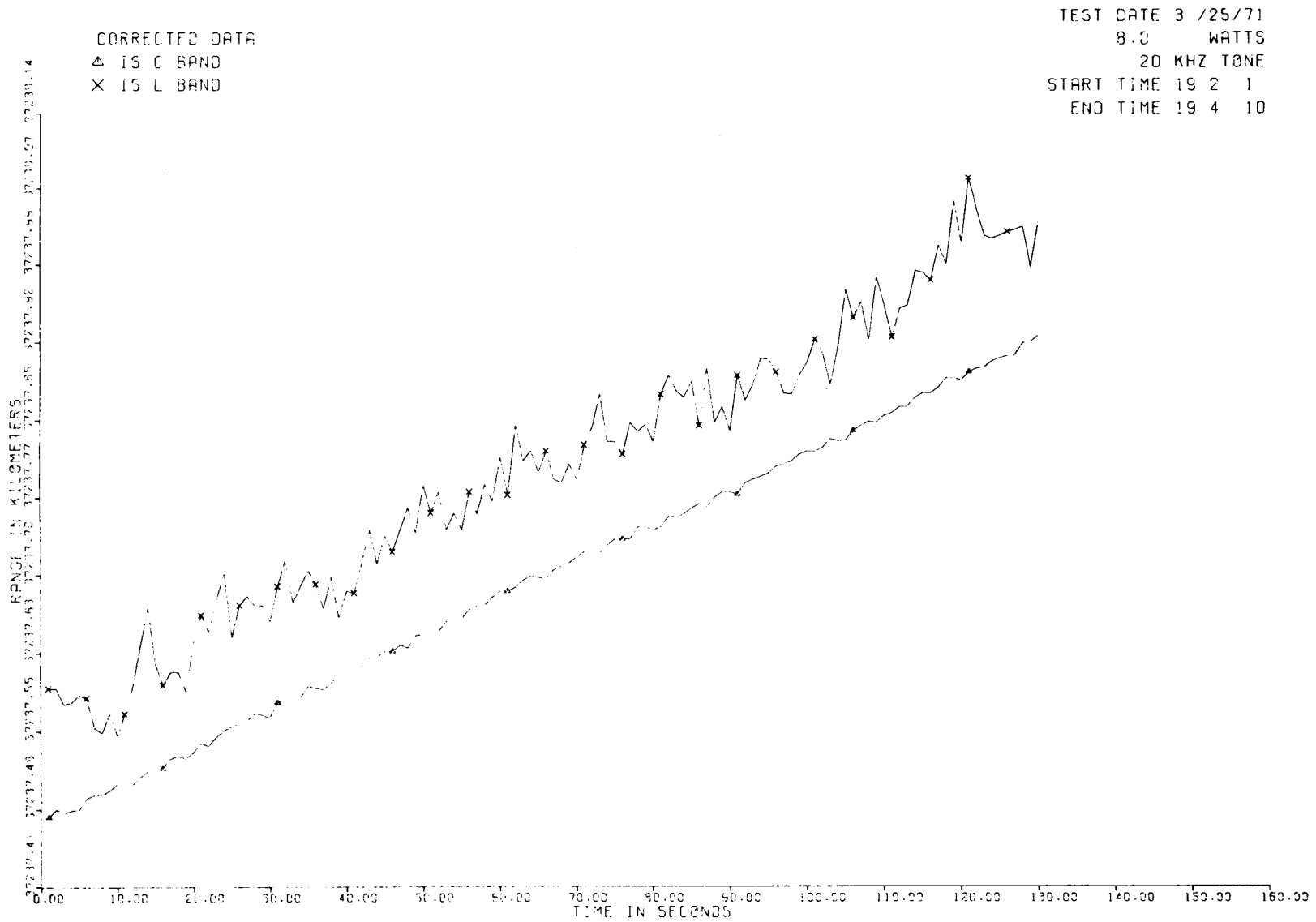

Figure 3.5 Detailed Ranging Plots, Corrected Data

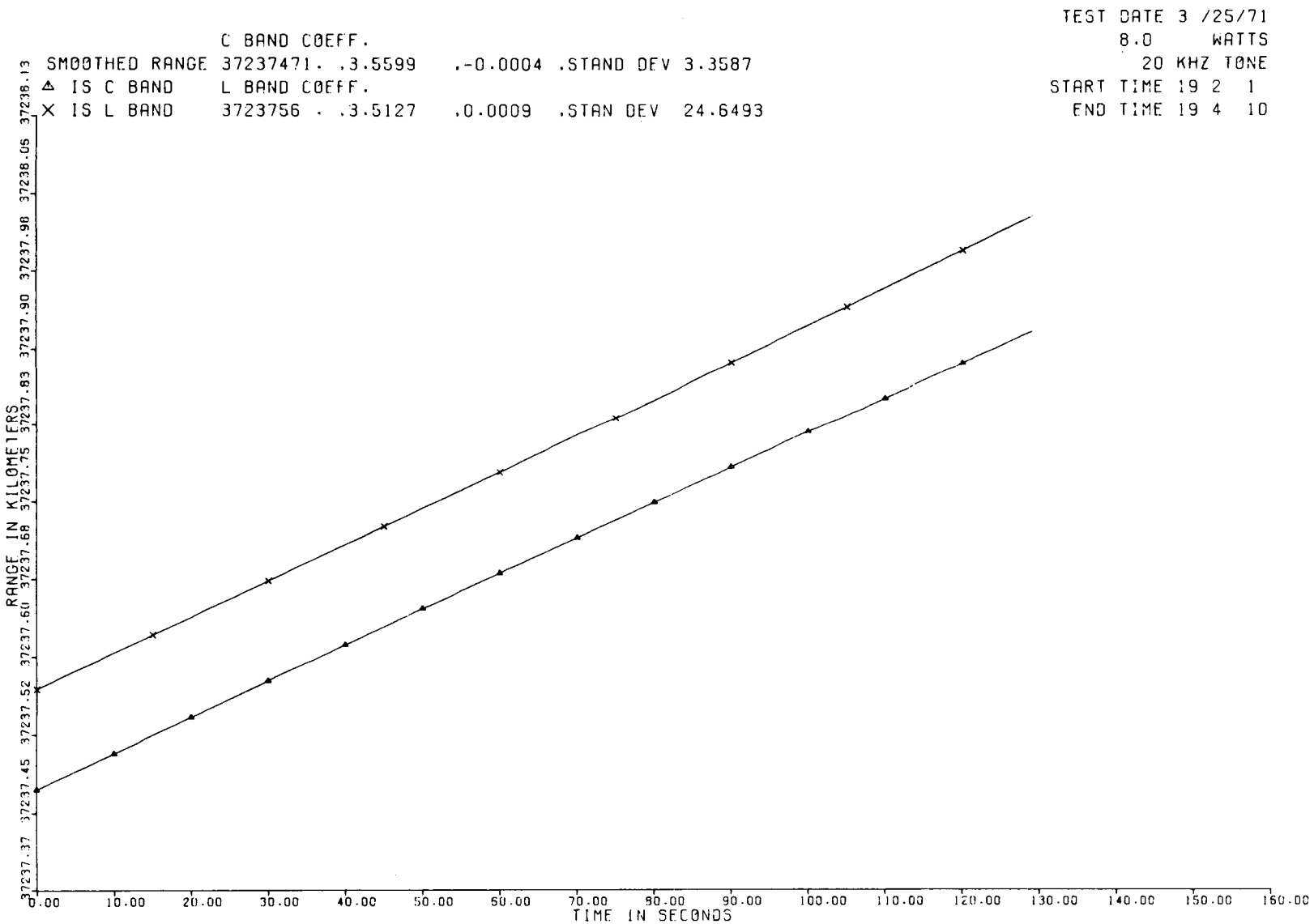

Figure 3.6 Detailed Ranging Plots, Smoothed Range

TABLE 3.1 SIMULTANEOUS RANGING ON ATS-5 (25 MARCH 1971)

Hrs.	Min.	Sec.	L-Band Xmtr. Power	Range in Meters			Standard Deviation in Meters	
				Ephemeris Prediction	C-Band	L-Band	C-Band	L-Band
18	42	02	1 KW	37233730	37233405	37233530	4.20	4.52
18	46	03	250W	37234516	37234232	27234378	4.79	4.13
18	50	30	64W	37235309	37234999	37235148	3.66	4.08
18	54	20	32W	37236180	37235913	37236064	3.04	4.86
18	58	04	16W	37236942	37236651	37236796	3.86	8.12
19	02	01	8W	37237758	37237471	37237560	3.35	24.65
19	06	02	4W	37238603	37238319	37238224	3.60	52.01

the velocity and acceleration coefficients of the second-degree polynominal curve. The values of standard deviation illustrate the aforementioned performance degradation due to low signal levels.

Another degradation caused by low signal levels is seen in the last two measurements listed in Table 3.1. The differential in range readings between C-band and L-band averages about 140 meters at L-band transmitting levels above 15 watts, but at 8 watts and 4 watts this differential decreases and even occasionally reverses sign. This phenomenon is caused by the noise response phase characteristic of the ranging tone filter in the equipment. The filter has since been redesigned to correct this biasing condition.

With this understanding it is seen that, in general, the L-band ranging averages approximately 140 meters greater than the C-band. This differential is caused by a discrepancy in the calibration "zero-set" for the L-band system. The range from the L-band antenna to the collimation tower equipment antenna is 3460 meters. This is equivalent to a two-way range reading of about 23070 nanoseconds. The collimation tower equipment delay of 60 nanoseconds must be added to this figure, and the satellite delay of about 450 nanoseconds must be deducted. This yields a one-way calibration setting of 11,340 nanoseconds. However, the data was obtained using a calibration setting of 11,730 nanoseconds, and thus the L-band range readings are approximately 120 meters too long. Therefore, it is seen that the L-band range measurement agrees very well with that of the C-band.

Comparison of the C-band ranging measurement with the ephemeris predictions reveals a bias of about 250 to 300 meters. The ephemeris range is longer than the C-band measurement. Inquiry has revealed that the antenna location used for ephemeris calculations is approximately 17 meters north and 89 meters west of that used by the ATS project. If the ephemeris program actually is in error, a very small amount of the observed differential is explained. However, other constants in the ephemeris program, such as the value used for Earth radius at Mojave could also be contributing to the bias. Finally, a differential between Rosman and Mojave range readings could also be causing the ephemeris determination of S/C location to be displaced sufficiently to cause the 250- to 300-meter discrepancy at Mojave. For example, averaging the readings from two or more stations could easily cause the predicted position of the satellite to be displaced from Mojave's range reading by the observed variance. This discrepancy will be further investigated at a later point in the program.

3.3.2 Position Location Determination

Data for this experiment was collected by ranging on the ATS-1 satellite with the ATSR C-band ranging system and on the ATS-5 satellite with the L-band ranging system. Each test run collected three minutes of concurrent data from each satellite. The first step in the reduction of these readings was to obtain the emphemeris data for the satellite latitude, longitude, geocentric elevation, and slant range for both ATS-1 and ATS-5 during the test interval. From this and the measured data, position location scatter plots can be made to locate the measuring point, which in this case is the Mojave ground station.

The ephemeris data magnetic tapes had not been received at this time, but several of the ephemeris printouts were available. For the first position location test run on 25 March 1971 (181306Z - 181557Z) three points, one at the beginning, one in the middle, and one at the end of the test run, were extracted and manually entered into the position location computer program. From this, the plots shown in figures 3.7 and 3.8 were computed. The first plot (figure 3.7) takes the slant range ephemeris data and attempts to return to the station, which was the point from which this ephemeris data was calculated. The second plot (figure 3.8) substitutes the actual range measurements received at these three times and attempts to locate the point from which the range measurements were performed. The results showed that the ephemeris data returned to within 87 meters of the station and the measured data was within 309 meters.

Considering that this is a first try with this data and this program, these results are very good. Errors are expected to exist due to the finite accuracy of the input data; such as satellite and station location from the ephemeris data being given to only three decimal places and to the round off differences in program conversion constants. With continuing upgrading in this computer program, confidence in the position location test results will be greatly improved.

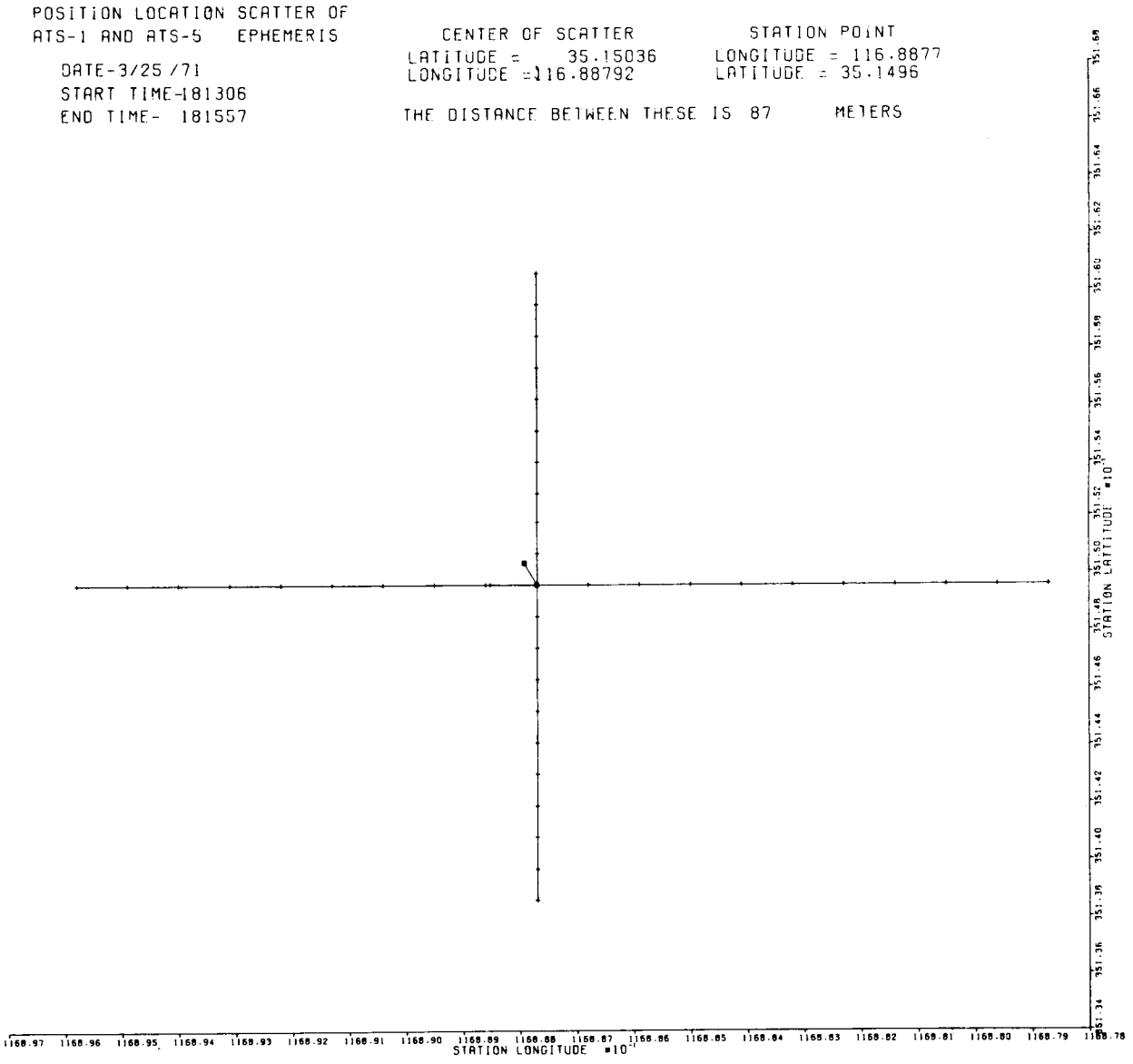

Figure 3.7 Position Location Plots, Ephemeris Data

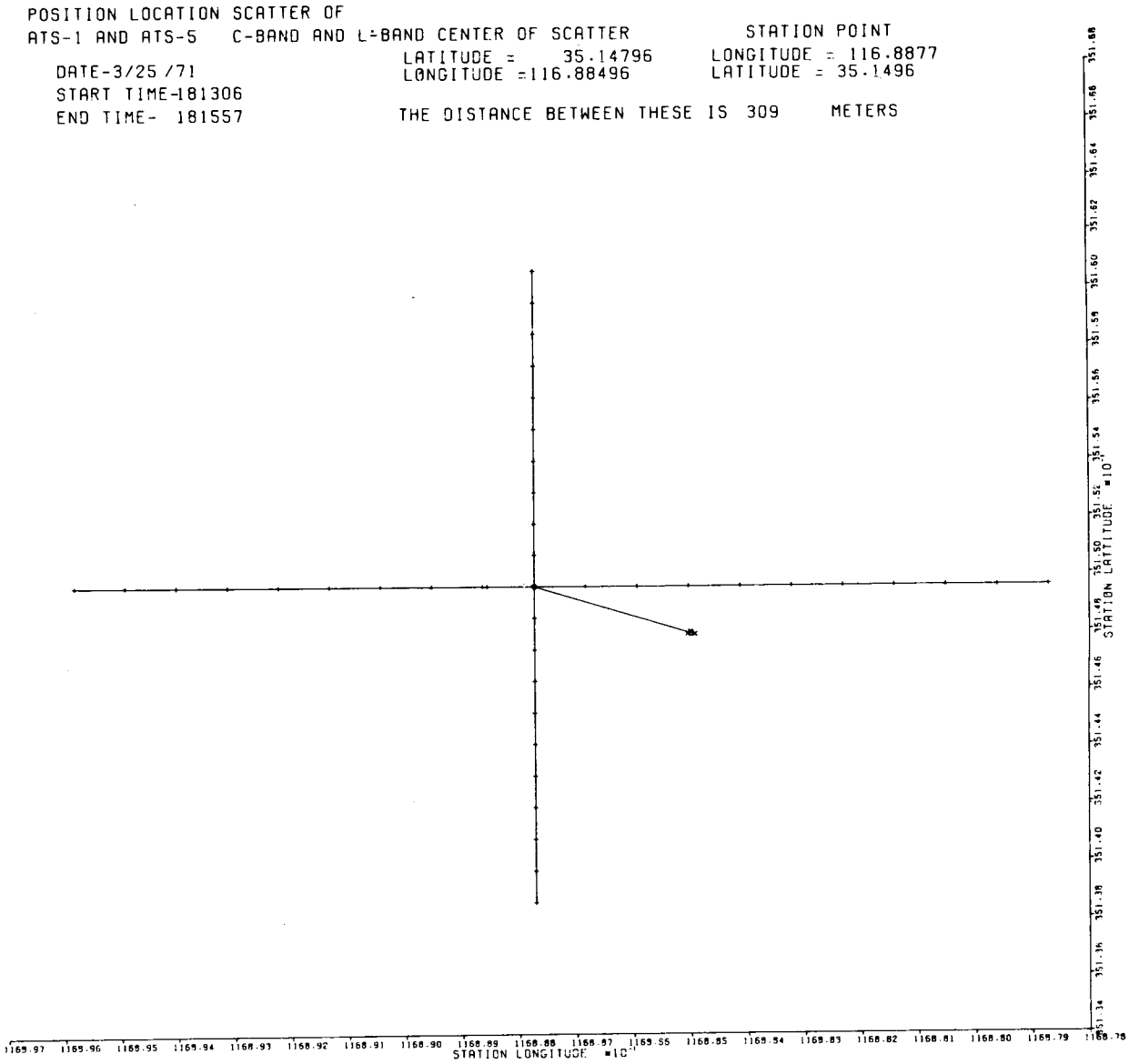

Figure 3.8 Position Location Plots, Measured Data

APPENDIX A

DETAILED RANGE DEMODULATOR ANALYSIS

RANGE DEMODULATOR

The range demodulator utilizes information in the baseband signal (from the carrier track receiver) to reconstruct either the 4-kHz or the 20-kHz propagation-delayed range tone. The delay between this replica and the corresponding reference tone is periodically measured to obtain a sequence of estimates of the total propagation delay. The measurement and display/printout period corresponds to the spin period of the ATS-5 spacecraft.

Because of the ATS-5 spin, the range information in the baseband signal is contained in periodic bursts. The tones contained in these bursts are corrupted by additive, wideband noise and by distortion introduced in the tracking receiver. This distortion is of concern during the initial portion of each burst interval as the tracking receiver attempts to acquire the carrier. This distortion, along with reduced signal levels, severely restricts the range information available during the initial and final portions of each tone burst. These portions are therefore discarded, and the reconstruction of the range tones is based solely on the remaining 40 msec. of each burst, during which time the baseband signal-to-noise density power ratio is reasonably constant at approximately 48 dB-Hz. This value is based upon the expected satellite-to-aircraft link conditions as given in the link calculation table. As was done for the carrier track loop, a 3-dB margin has been introduced, reducing the minimum input S/N_o, for design purposes, to 45 dB-Hz over each 40-msec. viewing interval.

The delay between the reconstructed tone (actually a square wave) and the baseband signal during each 40 msec. viewing interval is measured by counting the time in increments of 20 nsec. between the crossover points of the two tones; that is, the time from one signal exceeding its mean value to the other signal exceeding its mean value. The crossover points for the baseband tone are obtained by hard-limiting prior to the delay measurement. One such delay measurement is obtained for each cycle of the range tone, or once every 50 usec. for the 20-kHz tone and once every 250 usec. for the 4-kHz tone.

These measurements are used to correct the delay of the reconstructed tone. However, since the measurements are noisy, the reconstructed signal is shifted by only a small fraction of the delay obtained in each measurement. In this way the measured values of delay error are averaged and the variations due to noise are reduced. The measurements and corrections occur sequentially at the 20-kHz or 4-kHz rates over the 40-msec. viewing intervals. With $\hat{\tau}_n$ the delay (with respect to, say, the reference tone) of the reconstructed tone at the nth instant, and the delay of the received tone at the nth instant, the delay of the reconstructed tone at the $(n+1)^{th}$ instant, neglecting the 2-nsec. measuring quantization and a similar 2-nsec. quantization in the delay of the reconstructed tone, will be:

$$\hat{\tau}_{n+1} = \hat{\tau}_n + a(\tau_n - \hat{\tau}_n) \tag{1}$$

The coefficient, "a," expresses the fact that the amount of correction is only proportional to the measured error. For the 20-kHz tone, the coefficient value used is $a = 2^{-11} = 4.88 \times 10^{-4}$ while for the 4-kHz tone, the coefficient value used is $a = 2^{-7} = 7.82 \times 10^{-3}$.

The propagation delay (range) output readings are based on the delay, $\hat{\tau}_n$, at the end of each 40-msec. viewing interval. These "final values" themselves form a sequence which can be represented by the recursive relations:

$$\hat{\tau}^*_{\ell+1} = \hat{\tau}^*_{\ell} + V_{\ell} + \Delta_{\ell+1} \tag{2a}$$

$$V_{\ell+1} = V_{\ell} + b\ \Delta_{\ell+1} \tag{2b}$$

Where $\hat{\tau}^*_{\ell}$ is the last $\hat{\tau}$ in the ℓ^{th} viewing interval and $\Delta\ell$ is the change in $\hat{\tau}$ over the ℓ^{th} viewing interval.

The variable, V_{ℓ}, is simply the accumulation of the corrections, Δ, as is indicated by (2b), and serves as an estimate of the change in delay from the end of one viewing interval to the beginning of the next interval. The coefficient b is adjustable by means of a plug-in patch board. The value of this coefficient used was 2^{-3}, or 0.125.

Since the viewing interval is relatively short (40 msec.), the tone delay (range) and all its derivatives will be very nearly constant over a viewing interval. Thus, the tone delay and its derivatives can be represented by sequences of their values at each viewing interval. The change in delay of the reconstructed tone during

the ℓ^{th} viewing interval, $\Delta\ell$, can be expressed in terms of the initial estimated delay and the ℓ^{th} input delay and its derivatives, using equation:

$$\Delta\ell = (\tau^*_\ell - \hat{\tau}^*_{\ell+1} - V_{\ell-1})(1 - K_p) - K_v \dot{\tau}^*_\ell - K_a \ddot{\tau}^*_\ell + N_\ell \qquad (3)$$

where τ^*_ℓ, $\dot{\tau}^*_\ell$, $\ddot{\tau}^*_\ell$, are, respectively, the values of the propagation delay and of its first and second derivatives during the ℓ^{th} viewing interval. N_ℓ is the error due to noise and other uncertainties. (The effects of the higher order derivatives are negligibly small for ranging to vehicles having aircraft performance capabilities or less, and have been omitted.)

For 4-kHz tone ranging:

$$\begin{aligned} K_p &\cong 0.287 \\ K_v &\cong 5.70 \times 10^{-3} \\ Ka &\cong 3.38 \times 10^{-5} \end{aligned} \qquad (4a)$$

and for 20-kHz tone ranging:

$$\begin{aligned} K_p &\cong 0.677 \\ K_v &\cong 3.30 \times 10^{-2} \\ K_a &\cong 6.95 \times 10^{-4} \end{aligned} \qquad (4b)$$

Equations (2) and (3) can be combined to obtain the relationship between the sequence of range measurements and the sequences of the actual range and its first two derivatives and the sequence of uncertainties. Expressed recursively:

$$\hat{\tau}^*_\ell = [1 + K_p - b(1 - K_p)]\ \hat{\tau}^*_{\ell-1} - Kp\ \hat{\tau}^*_{\ell-2} + (1 - K_p)\ [\tau^*_\ell - (1-b)\ \tau^*_{\ell-1}] \qquad (5a)$$

$$- K_v\ [\dot{\tau}^*_\ell - (1-b)\ \dot{\tau}^*_{\ell-1}] - K_a\ [\ddot{\tau}_\ell - (1-b)\ \ddot{\tau}_{\ell-1}] + N_\ell - (1-b)\ N_{\ell-1}$$

Expressed as a Z-transform: (5b)

$$\hat{\tau}^* = \frac{(1 - K_p)\ Z\ (Z - 1 - b)}{Z^2 - [1 + K_p - b\ (1 - K_p)\ Z] + K_p} \left\{ \tau^* - \frac{1}{(1 - K_p)} [K_v\ \dot{\tau}^* + K_a\ \ddot{\tau} - N] \right\}$$

The sequences, τ^*, $\dot{\tau}^*$ and $\ddot{\tau}^*$ represent sample values taken on the propagation delay, τ, and its first two derivatives, $\dot{\tau}$ and $\ddot{\tau}$, at a rate equal to the spin rate of the spacecraft; i.e., about one sample per 790 msec. Frequency response characteristics can therefore be obtained from (5b) by setting $Z = \exp(-j\ .79\ \omega)$.

A bound on the error due to changes in range can be obtained from (5b) by placing upper bounds on $\dot{\tau}$ and $\ddot{\tau}$.

The first derivatives of propagation delay, $\dot{\tau}$, due to spacecraft motion has negligible effect. For the aircraft, $|\dot{\tau}| \leq 2$ usec./sec. has been assumed.

The second derivative of propagation delay, $\ddot{\tau}$, has a component due to the spin of the spacecraft of about 0.31 usec./sec.^{2} and a component due to the aircraft of magnitude less than 0.1 usec./sec.^{2} (50 ft/sec.^{2} acceleration). So 0.21 usec./sec.^{2} $\leq |\ddot{\tau}| \leq$ 0.41 usec./sec.^{2}.

The steady-state error due to $\dot{\tau}$ and $\ddot{\tau}$ can be obtained from (5b) by substituting the bounds on $\dot{\tau}$ and $\ddot{\tau}$ and setting Z=1. This results in:

$$\epsilon_M \leq \frac{1}{(1 - K_p)} \quad (2 \times 10^{-6} K_v + 0.41 \times 10^{-6} K_a)$$

or, for the 4-kHz tone, $\epsilon_M \leq$ 17 nsec., while for the 20-kHz tone, $\epsilon_M \leq$ 204 nsec.

The sequence $\{N_\ell\}$ contains uncertainties due to temperature variations and aging, which have strong sample-to-sample correlation, and uncertainties due to the baseband signal-to-noise power ratio and quantization, which produce essentially uncorrelated sample values. The long term uncertainties in $\{N_\ell\}$ appear one-for-one in the range output sequence, as would be expected. The principal long term uncertainty allowance in the range demodulator has been made for the analog filters. It will be seen later that a standard deviation of less than 125 nsec. has been estimated for the 4-kHz filter and less than 25 nsec. for the 20-kHz filter.

The reconstructed tones are time quantized to $\pm$10 nsec. Since these errors are uniformly distributed in amplitude over the $\pm$10-nsec. interval, the quantization uncertainty has a standard deviation of $20/\sqrt{12} = 5.8$ nsec. This quantization uncertainty also appears one-for-one in the range output readings.

The composite baseband signal consists of the ranging tone (signal), A sin $2\pi F[t - \tau(t),]$ plus additive, wideband, zero mean noise, $v(t)$. The n^{th} member of the input delay sequence, τ_n, is based on the n^{th} crossover point, so the n^{th} delay error, $\delta_n \triangleq \tau(t) - \tau_n$ with v_n, the noise voltage at the n^{th} crossover, is the minimum magnitude solution to:

$$A \sin 2\pi F \delta_n = v_n \tag{6}$$

or

$$\delta_n = \frac{1}{2\pi F} \sin^{-1}\left(\frac{v_n}{A}\right)$$

For $v_n \ll A$

$$\delta_n \cong \frac{1}{2\pi F}\left(\frac{v_n}{A}\right) \tag{7}$$

Since (7) is linear, the spectral densitities of δ and v are similar, and are related by (from (7)):

$$\eta_{(f)} = \frac{\eta_v(f)}{2\pi F A} \tag{8}$$

The processing bandwidth is very much less than the bandwidth of v (t), so the sample values $\{\delta_n\}$ can be treated as being essentially uncorrelated. These sample values are obtained at a rate equal to the range tone frequency, F, so $\{\delta_n\}$ is essentially uniformly distributed over the frequency interval $[-F/2 \text{ to } F/2]$, and therefore the variance of $\{\delta_n\}$, σ_δ^2, is given by:

$$\sigma_\delta^2 = F \quad \eta_s^2 \tag{9}$$

But the baseband signal (tone)-to-noise power density is:

$$\left(\frac{S}{N_o}\right) = \frac{A^2}{2\eta_v^2} \tag{10}$$

So, from (8), (9) and (10)

$$\sigma = \frac{1}{2\pi\sqrt{F}}\left(\frac{S}{N_o}\right)^{-1/2} \text{ Seconds} \tag{11}$$

This variance is a sort of RMS value for the noise-induced errors in the delay measurements used in reconstructing the propagation-delayed range tone. A number of these measurement errors are obtained over each 40-msec. viewing interval, resulting in a sequence of uncertainties - a portion of $\{N_\ell\}$ in equation (3) - produced at the spacecraft spin rate. Each member of this random sequence depends only upon those measurement errors which occurred during one of the viewing intervals, so the members of this sequence are uncorrelated. It is shown in Addendum 2 that the variance of this noise sequence, σ_N^2, obtained by considering the process of equation (1), is related to the variance of the individual measurement errors, σ_δ^2, by:

$$\sigma_N^2 = \frac{[1 - (1 - a)^{2M}]}{2 - a} \quad a\ \sigma_\delta^2 \tag{12}$$

where "a" is the coefficient in equation (1) and M is the number of delay measurements made in a 40-msec. viewing interval: 160 for the 4-kHz tone and 800 for the 20-kHz tone.

This uncorrelated, random sequence, which represents the uncertainties obtained during each sequential viewing interval, is introduced into the final output readings via the process of equations (5a) or (5b). The estimated process modified the effect of the "input" uncertainties because of the "memory" or "filtering" involved. The variance of the noise-induced uncertainties in the output readings, σ_n^2, is given by (see addendum 2):

$$\sigma_{on}^2 = \frac{[2 - b - (2 - 3b) K_p]}{(1 - K_p)^2 \quad [2 - b + (2 + b) K_p]} \quad \sigma_n^2 \tag{13}$$

Combining equations (11), (12) and (13):

$$\sigma_{on}^2 \quad \frac{a [1 - (1 - a)^{2M}] \qquad [2 - b - (2 - 3b) K_p]}{8 \quad \pi^2 F (2 - a) (1 - K_p)^2 \quad [2 - b + (2 + b) K_p]} \quad \left(\frac{S}{N_o}\right)^{-1} \tag{14}$$

Using the values given for a, b, M and F (Addendum 2) equation (14) yields, with $(S/N_o) \leq$ 45 dB (about 3.16×10^4 Hz), for 4-kHz tone ranging:

$$\sigma_{on}^2 \cong 1.63 \times 10^{-8} \left(\frac{S}{N_o}\right)^{-1} \leq 5.15 \times 10^{-13} \text{ sec}^2 \tag{15a}$$

and for 20-kHz tone ranging:

$$\sigma_{on}^2 \cong 3.51 \times 10^{-10} \left(\frac{S}{N_o}\right)^{-1} \leq 1.11 \times 10^{-14} \text{ sec}^2 \tag{15b}$$

The total uncertainties introduced by the analog filter, the quantization, and the baseband noise have standard deviation of:

For 4 -KHz tone ranging:

$$\sigma^2 < [(125)^2 + (5.8)^2 + 5.15 \times 10^5] \times 10^{-18} \cong 53 \times 10^{-14} \text{ sec}^2$$

or

$$\sigma < 730 \text{ nsec} \tag{16a}$$

For 20-kHz tone ranging:

$$\sigma^2 < [(25)^2 + (5.8)^2 + 1.11 \times 10^4] \times 10^{-18} \cong 1.17 \times 10^{-14} \text{ sec}^2$$

or

$$\sigma < 108 \text{ nsec} \tag{16b}$$

It has been mentioned that the processing being performed by the range demodulator is a form of "averaging." The demodulator attenuation of noise components increases with increased difference between the frequency and the particular range tone frequency being used. That portion of the noise spectrum in the neighborhood of the tone frequency has strong sample-to-sample correlation and is therefore attenuated less. In fact, this strong sample-to-sample correlation will be exhibited by noise with spectrums centered about any integer (or zero) multiple of the tone frequency. This is the aliasing effect seen in discrete time filters.

A second minor problem that should be discussed at this point concerns the signal-to-noise power ratio (not noise density) at the input to the hard limiter. A linear approximation to the delay error, based on the signal amplitude being large with respect to the noise amplitude, was previously made in equation (7). The validation of this approximation is desirable for a reason other than the simplification of the mathematics, although the linearity of (7) is welcomed. The prime reason for requiring a high signal-to-noise ratio at this point is that the rate-of-change of the tone signal will be larger at the crossover point with a high S/N than with a low S/N, resulting in a delay uncertainty with variance less than proportional to $(S/N)^{-1}$. This is the effect which gave rise to the $\sqrt{2}$ in equation (11), and is the familiar 3-dB "improvement" in signal-to-noise ratio obtained by hard limiting with high input signal-to-noise ratios.

Both the aliasing problem and the problem of obtaining a signal-to-noise ratio into the limiter sufficiently high to obtain the 3-dB "improvement" are handled by the use of analog filters at the input to the hard limiters.

Such filters will, of course, introduce a phase uncertainty and a phase error or both. Every frequency filter requires some sort of frequency or time reference since it must operate on signals according to their frequency or period, and these references vary with temperature, time, humidity, etc. Active RC filters are used in the range demodulator, so the time references are RC time constants. Using metal film resistors ("C" temperature coefficient) and mica capacitors ("F" temperature coefficient), the time constants have an error with a mean of 35 ppm/^{o} C and a standard deviation of about 35 ppm/^{o} C. Each filter will contain a number of these time constants, and it is highly unlikely that all would vary the same. However, for design purposes, this has been assumed. This worst case situation is also easy to work with since an equivalent situation is obtained by fixing the time constants (and the filter characteristics, except for a scale factor) and changing the tone frequency.

Obviously, it is desirable for the phase slope to be a minimum at the tone frequency. In other words, the filters should be bandpassed with geometric center at the tone frequency, the wider the better as far as phase stability is concerned.

The filter characteristics selected were second-order Butterworth. The same characteristic, relative to the center frequency, was used for both tones:

$$G(S) = \frac{6.4 \quad \omega_o^2 \quad S^2}{(S^2 + 0.406 \quad \omega_o S + 0.560 \quad \omega_o^2)(S^2 + 0.725 \quad \omega_o S + 1.785 \quad \omega_o^2)} \qquad (17)$$

where

$$\omega_o = 2\pi \quad (4 \times 10^3) \text{ or } 2\pi \quad (20 \times 10^3)$$

This characteristic results in an output signal-to-noise power ratio of somewhat better than 3 dB with an input signal-to-noise power density ratio of 45 dB for the 20-kHz filter, and, or course, 5 times this for the 4-kHz filter. The attenuation in the vicinity of $\epsilon \omega_o$, $\epsilon = 0, 2, 3$, etc., is such that the increase in noise in the range measurements due to aliasing is less than 0.33 dB.

Using the time-constant sensitivities given above, the phase uncertainty with $\pm 20^{\circ}$ C temperature uncertainty has a standard deviation of less than 25 nsec. for the 20-kHz tone, and 125 nsec. for the 4-kHz tone.

ADDENDUM 1: Dynamic Response

The response of the range demodulator over a 40-msec. viewing interval can be obtained from the recursive relation of equation (1). Define the n^{th} error:

$$e_n \triangleq \tau_n - \hat{\tau}_n \tag{A-1}$$

Combining (1) and (A-1), obtain the recursive relation for the error sequence:

$$e_{n+1} = (1 - a)\ e_n + (\tau_{n+1} - \tau_n) \tag{A-2}$$

The error with an initial positive error is obtained from (A-2) with $\tau_{n+1} = \tau_n$; n = 0, 1, - - - -:

$$e_n^{(o)} = e_o (1 - a)^n \tag{A-3}$$

The error with a constant velocity input is obtained from (A-2) with

$e_o = \tau_o = 0$ and $\tau_{n+1} = \tau_n + \dot{\tau}_o/F$:

$$e_n^{(1)} = \dot{\tau}_o \frac{1}{a\ F} \left[1 - (1 - a)^n\right] \tag{A-4}$$

The error with a constant acceleration input is obtained from (A-2) with $e_o = \tau_o = o$ and $\tau_{n+1} = \tau_n + n\ \ddot{\tau}_o/2\ F^2$

$$e_n^{(2)} = \ddot{\tau}_o \frac{1}{2\ a^2\ F^2} \left[a_n + 1 + (1 - a)^n\right] \tag{A-5}$$

Since the viewing interval is short, the range, even with high performance aircraft, will be approximately constant over the viewing interval, as will the first- and second derivatives of range. The effects of higher order derivatives are negligible. Thus, the error sequence over a viewing interval can be obtained very closely from equations (A-3), (A-4), and (A-5) and the range and its first two derivatives.

The error at the end of the 40-msec. viewing interval is obtained by setting $n = 40 \times 10^{-3}$ F; i.e., the number of iterations in the interval. The error at the end of the interval is then:

$$e_M \cong K_p\ e_o + K_v\ \dot{\tau}_o + K_a\ \ddot{\tau}_o$$

Where

$$K_p \triangleq (1 - a)^M \qquad \text{(A-6)}$$

$$K_v \triangleq \frac{1}{a F} \left[1 - (1 - a)^M\right]$$

$$K_a \triangleq \frac{1}{2 a^2 F^2} \left[a M - 1 + (1 - a)^M\right]$$

$$M \triangleq 40 \times 10^{-3} F$$

A useful approximation is:

$$(1 - a)^M \cong \exp(-a M) \qquad \text{(A-7)}$$

for a $M > 1$ and a $\ll 1$.

Numeric values for the coefficients of (A-6) can be obtained either directly or by use of the approximation of (A-7).

For 4-kHz tone ranging, $F = 4 \times 10^3$ and $a = 7.825 \times 10^{-3}$, so:

$$K_p \cong 0.287$$
$$K_v \cong 5.70 \times 10^{-3} \qquad \text{(A-8)}$$
$$K_a \cong 1.69 \times 10^{-5}$$

For 20-kHz tone ranging, $F = 2 \times 10^4$ and $a \cong 4.88 \times 10^{-4}$, so:

$$K_p \cong 0.677$$
$$K_v \cong 3.30 \times 10^{-2} \qquad \text{(A-9)}$$
$$K_a \cong 3.48 \times 10^{-4}$$

ADDENDUM 2: Noise Response

Each delay error measurement made during a 40-msec. viewing interval is corrupted (additively) by a member of the random sequence $\{\delta_n\}$. The members of this sequence have zero mean variance, σ_δ^2, and are uncorrelated. In other words:

$$\langle \delta_n \rangle = 0$$

$$\langle \delta_n \quad \delta_M \rangle = \begin{cases} \sigma_\delta^2 & \text{for } n = M \\ 0 & \text{for } n \neq M \end{cases} \qquad \text{(B-1)}$$

Where $\langle \delta_n \rangle$ denotes the expected value of δ.

The delay error sequence due to one such "noise" sequence is, from (1), a solution to:

$$e_{n+1} = (1 - a) \; e_n + a \; \delta_n \qquad \text{(B-2)}$$

The error at the end of the viewing interval due to the errors which occurred only during that viewing interval is obtained from (B-2) by setting $e_o = 0$ and solving for e_M, where $M = 40 \times 10^{-3}$ F; i.e., the number of iterations in the viewing interval. The resulting sequence is: $e_o = 0$, $e_1 = a \; \delta_o$, $e_2 = (1 - a) \; a \quad \delta_o + a \; \delta_1$, etc.,

so

$$e_M = a \sum_{i = 0}^{M-1} (1 - a)^{M-1-i} \quad \delta_i \qquad \text{(B-3)}$$

The variance of e_M, σ_n^2 using (B-1) and (B-3) is:

$$\sigma_n^2 \triangleq \langle e_M \rangle = \sigma_\delta^2 \; a^2 \sum_{i = 0}^{M - 1} (1 - a)^{2 (M - 1 - i)} \qquad \text{(B-4)}$$

or

$$\sigma_n^2 = \sigma_\delta^2 \; a \; \frac{[1 - (1 - a)^{2M}]}{(2 - a)} \qquad \text{(B-5)}$$

The final error values, e_M, themselves form a sequence, $\{e_{M\ell}\}$, of values at a rate equal to the spin rate of the spacecraft. This noise sequence appears in the sequence of output readings modified by the process with Z - transform, from equations (2) and (3), setting τ, $\dot{\tau}$, $\ddot{\tau} = 0$:

$$Z \hat{\tau}^* = \hat{\tau} + V + Z\Delta$$

$$Z V = V + Z b \Delta$$

$$Z \Delta = Z e_M - (\hat{\tau}^* + V)(1 - K_p) \qquad \text{(B-6)}$$

Combining these equations yields the noise transfer function:

$$\hat{\tau}(Z) = \frac{Z (Z - 1 + b)}{Z^2 - [1 + K_p - b (1 - K_p)] Z + K_p} e_M \triangleq G_N (Z) e_M \qquad \text{(B-7)}$$

Since the input noise samples are essentially uncorrelated due to the relatively long (790 msec.) time between samples, they can be considered as samples taken on a continuous noise signal with spectrum of $\eta = 0.79 \sigma_n^2$ (sec.^{2}/Hz) for $|f| \leq f_o = (2 \times .79)^{-1}$, zero otherwise.

The frequency response of the process, G(f), can be obtained from the Z - transform, $G_n(Z)$, by setting $Z = \exp [j(.79)(2 \pi f)]$. The variance of the output noise is then:

$$\sigma_{on}^2 = \int_{-\infty}^{\infty} |G(f)|^2 \eta (f) \, df = 0.79 \sigma_n^2 \int_{-f_o}^{f_o} G(f) \overline{G(f)} \, df \qquad \text{(B-8)}$$

where $\overline{G(f)}$ is the complex-conjugate of G(f).

This integration can be carried out in the independent variable Z using the previous definition and its derivative:

$$dZ = j (0.79)(2 \pi) Z \, df \qquad \text{(B-9)}$$

The limits of the integration then become $Z = \pm \pi$, and the path of the integration is along the unit circle in the complex - Z plane.

So, with $\overline{G(Z)} = G(Z^{-1})$

$$\sigma_{on}^2 = \frac{\sigma_n}{j 2 \pi} \oint G(Z) G(Z^{-1}) Z^{-1} \, dZ \qquad \text{(B-10)}$$

The contour integral of (B-10) can be evaluated by the method of residues:

$$\oint f(Z) \, dZ = j 2 \pi \sum \text{residues of } f(Z) \text{ in the unit circle} \qquad \text{(B-11)}$$

G (Z) has two singularities, the roots of:

$$Z^2 - [1 + K_p - b (1 - K_p)] Z + K_p$$

$$Z_1, Z_2 = 1/2 \left[(1 - b) + (1 + b) K_p \pm \sqrt{(1-b)^2 - 2 (1 + b^2) K_p + (1 + b)^2 K_p^2}\right] \qquad \text{(B-12)}$$

For stability, let Z_1 and Z_2 lie within the unit circle. So:

$$G_n(Z)\,G_M(Z^{-1})\,Z = \frac{[Z - (1-b)]\;[1-(1-b)\,Z]}{(Z - Z_1)(Z - Z_2)(1 - Z\,Z_1)(1 - Z\,Z_2)} \tag{B-13}$$

has only two singularities, at $Z = Z_1$ and $Z = Z_2$, within the unit circle ($|Z| < 1$). and

$$\sum \text{Residues} = \frac{[Z_1 - (1-b)]\,[1-(1-b)\,Z_1]}{(Z_1 - Z_2)(1 - Z_1^{\,2})(1 - Z_1\,Z_2)} + \tag{B-14}$$

$$\frac{[Z_2 - (1-b)]\;\;[1-(1-b)\,Z_2]}{(Z_2 - Z_1)(1 - Z_1\,Z_2)(1 - Z_2^{\,2})}$$

or

$$\sum \text{Residues} = \frac{(2 - 2b - b)^2\,(1 + Z_1\,Z_2) - 2\,(1-b)\,(Z_1 + Z_2)}{(1 - Z_1\,Z_2)\;[1 + (Z_1 + Z_2) + Z_1\,Z_2]\,[1 - (Z_1 + Z_2) + Z_1\,Z_2]} \tag{B-15}$$

But $Z_1\,Z_2 = k_p$ and $Z_1 + Z_2 = (1-b) + (1+b)\,k_p$, so, from (B-10), (B-11) and (B-15):

$$\sigma_{on}^{\,2} = \frac{[\,2 - b - (2 - 3b)\,K_p\,]}{(1 - K_p)^2\;\;[\,2 - b + (2 + b)\,K_p\,]}\;\;\sigma_n^{\,2} \tag{B-16}$$

Combining equations (B-5 and (B-15):

$$\sigma_{on}^{\,2} = \frac{a\,[1 - (1-a)^{2M}]\,[2 - b - (2 - 3b)\,K_p]}{(2 - a)\,(1 - K_p)^2\;[2 - b + (2 + b)\,K_p]}\;\;\sigma_\delta^{\,2} \tag{B-17}$$

GLOSSARY

Aliasing - For equally spaced data, the principal part of the aliased spectrum expresses contributions to the variance in terms of frequencies between zero and the Nyquist or folding frequency, all contributions from frequencies having the same principal alias and sign, having been combined by addition. The aliased spectrum repeats the principal part periodically with period 2fn.

ASCII - American Standard Code for Information Interchange.

Eight-level paper tape - one-inch-wide paper tape which is mechanically punched with up to eight holes per row. Information appears at hole sites where holes may or may not be punched. A character appears as a row of hole sites across the tape. A hole appears where a bit is a 1. Characters are placed along the length of the tape. The tape and hence the characters are scanned sequentially. A character row has punched in it a small hole which defines a character row and serves as a means for driving the tape.

Limiter Suppression - Signal suppression which results in a limiter due to a degraded signal to noise power ratio at the limiter input.

Minimum Lead Design - Control system utilizing the minimum lead required to achieve the loop frequency response. For additional information see "Synthesis of Feedback Control Systems With Minimum Lead Needed to Realize the Specified Frequency Response," a report by George S. Axelby of Westinghouse Electric Corporation.

OPLE - Omega Position Location Equipment which uses the worldwide Omega VLF radio signals as a means of establishing position location.